

Bayesian Matrix Factor Models for Demographic Analysis Across Age and Time

Gregor Zens*

International Institute for Applied Systems Analysis (IIASA)
Wittgenstein Centre for Demography and Global Human Capital (WIC)

December 12, 2025

Abstract

Analyzing demographic data collected across multiple populations, time periods, and age groups is challenging due to the interplay of high dimensionality, demographic heterogeneity among groups, and stochastic variability within smaller groups. This paper proposes a Bayesian matrix factor model to address these challenges. By factorizing count data matrices as the product of low-dimensional latent age and time factors, the model achieves a parsimonious representation that mitigates overfitting and remains computationally feasible even when hundreds of populations are involved. Informative priors enforce smoothness in the age factors and allow for the dynamic evolution of the time factors. A straightforward Markov chain Monte Carlo algorithm is developed for posterior inference. Applying the model to Austrian district-level migration data from 2002 to 2023 demonstrates its ability to accurately reconstruct complex demographic processes using only a fraction of the parameters required by conventional demographic factor models. A forecasting exercise shows that the proposed model consistently outperforms standard benchmarks. Beyond statistical demography, the framework holds promise for a wide range of applications involving noisy, heterogeneous, and high-dimensional non-Gaussian matrix-valued data.

Keywords: Bayesian Matrix Factorization; Statistical Demography; Non-Gaussian Data; High-Dimensional Statistics; Markov Chain Monte Carlo; Count Tensor Decomposition

*Contact: zens@iiasa.ac.at

1 Introduction

High-dimensional demographic data, covering both age and time dimensions across numerous subpopulations, are becoming increasingly common. Typical examples include subnational counts describing fertility, mortality, or migration patterns, often recorded annually and by single-year age groups. Statistical models of such fine-grained demographic data are used to forecast, track, and better understand demographic trends, in support of population projections and regional planning exercises.

When considering many subpopulations, modeling such multidimensional data is challenging due to the interplay of high dimensionality, heterogeneity across groups, and stochastic variation in small groups. As a result, demographic models must balance robustness to random fluctuations with sufficient flexibility to capture genuine demographic heterogeneity. In addition, they must be computationally efficient, as datasets may include hundreds or even thousands of subpopulations. This article develops a Bayesian framework that addresses these challenges.

As a motivating example, Fig. 1 shows a subset of outmigration count data from Austria, disaggregated by political district, age, sex, and year. A detailed description of the dataset is provided in Sec. 2. The small size of some subpopulations makes it difficult to separate meaningful demographic heterogeneity from noise based on the raw data alone. In such contexts, drawing reliable conclusions and gaining deeper insights into the underlying demographic process typically requires model-based approaches.

One family of models that has proven useful in this context relies on low-rank approximations, based, for example, on singular value decompositions (SVDs) or parametric factor models. Because demographic processes typically exhibit regularities across age and time, large datasets can often be described accurately using a small number of latent fac-

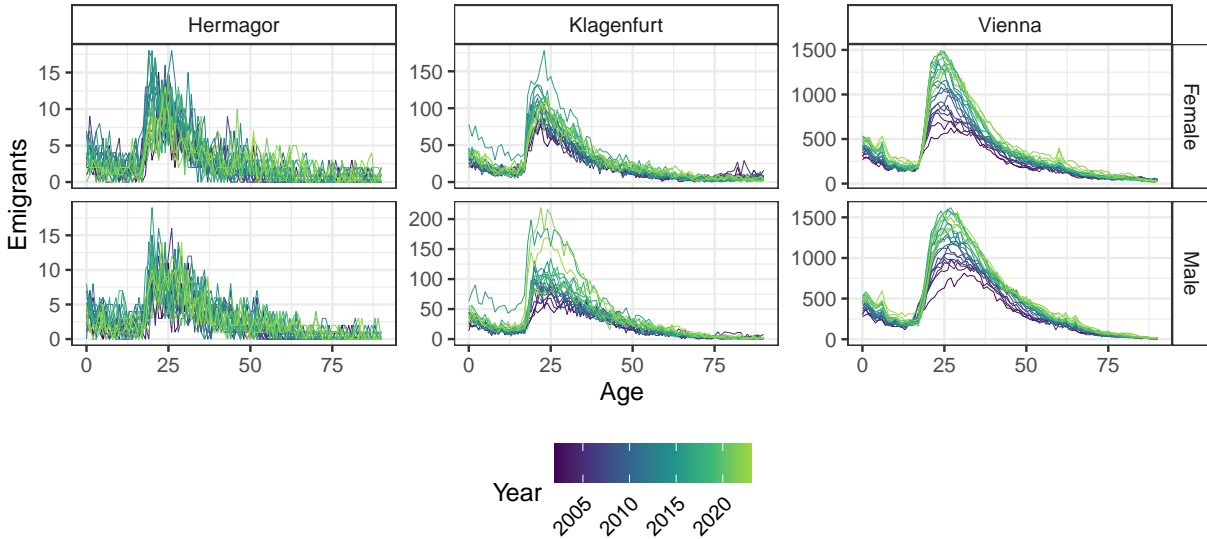


Figure 1: Outmigration counts by age (x-axis) and year (color) for six selected subpopulations, stratified by sex (rows) and district of origin (columns).

tors. Examples of such approaches include the SVD-based models of Lee & Carter (1992), Alexander et al. (2017), and Clark (2019), as well as related Bayesian frameworks (Czado et al. 2005; Wiśniowski et al. 2015; Zens 2025). However, existing demographic factorization methods typically target a single margin of the data, either extracting factors in the age dimension or the time dimension, while treating the other dimension(s) through high-dimensional loading parameters.

A key issue with this single-margin approach is that the number of parameters grows rapidly when data are measured across age, time, and many subpopulations. For instance, a time factorization of US county-level data covering around 3,000 counties and 100 age groups would require estimating 300,000 loading parameters per time factor. This creates computational bottlenecks and raises concerns about overfitting and statistical inefficiency, even when hierarchical or smoothing priors are employed for information sharing.

Recent advances in the statistical and machine learning literature on matrix and tensor factorizations offer a promising direction for addressing these challenges. Methods for fac-

torizing matrix- and tensor-valued data across multiple dimensions have been developed in various contexts, including econometric time series analysis (Wang et al. 2019; Billio et al. 2023; Qin et al. 2025) and the modeling of relational data (Hoff 2011*b*; Hoff 2015). These approaches demonstrate that simultaneous factorization across multiple margins can substantially reduce parameter counts while maintaining model flexibility. However, existing matrix and tensor factorization methods typically do not incorporate the domain-specific knowledge and constraints that are fundamental to demographic modeling, namely the need to handle overdispersed small counts while simultaneously accounting for prior information that demographic processes typically evolve smoothly across age and dynamically across time.

This article bridges this gap by developing a Bayesian low-rank matrix factor model specifically tailored for demographic analysis. The proposed model treats age–time data as matrix-valued observations for each subpopulation, decomposing each matrix into sets of latent age and time factors combined through subpopulation-specific loading matrices. This dual-margin factorization reduces the parameter count significantly, while the Bayesian framework enables fully probabilistic inference and uncertainty quantification. We apply the model to annual age- and sex-specific outmigration patterns across Austria’s 94 political districts from 2002 to 2023. Results demonstrate that the proposed approach achieves an effective balance between flexibility and robustness and provides structural insights into the underlying demographic process. A forecasting exercise further shows that the model consistently outperforms standard benchmarks in predictive accuracy, despite its much more parsimonious parameterization.

This work thus makes three main contributions to the literature on high-dimensional statistics for demographic applications. First, methodologically, we extend matrix factor-

ization techniques to the overdispersed count setting required for demographic data, while incorporating informative priors that enforce smoothness in the age factors and allow for dynamic evolution of the time factors. Second, we provide an in-depth empirical analysis using a high-dimensional Austrian district-level migration dataset — a particularly challenging application that combines structural breaks, sparsity, and heterogeneity. Third, we conduct a systematic comparison of various factorization strategies popular in statistical demography, demonstrating that simultaneous factorization across both age and time dimensions yields superior predictive performance while requiring only a fraction of the parameter count of traditional single-margin approaches.

The remainder of the article is structured as follows. Sec. 2 presents the motivating dataset and practical modeling problem. Sec. 3 reviews low-rank factorization approaches in the statistical and demographic literature. Sec. 4 introduces the proposed matrix factor model, prior specification, and posterior simulation algorithm. Sec. 5 details the real-data application and predictive exercise. Sec. 6 provides concluding remarks and discusses extensions and future research directions.

2 Motivating Application and Modeling Challenges

Demographic processes are frequently measured across three dimensions: age, time, and population, where we use the term ‘population’ as an umbrella term for various stratifications such as sex, geographical units, educational groups, or combinations thereof. This three-dimensional structure is universal in analyses of the three demographic components—mortality, fertility, and migration. As modern statistical offices increasingly provide such granular data, the statistical challenge lies in developing methods capable of modeling these high-dimensional datasets. Such models have important applications, ranging from

subnational population projections and regional infrastructure planning to healthcare resource allocation and assessments of pension system sustainability. The ability to track historical patterns and generate reliable forecasts thus directly supports evidence-based policy decisions at both regional and national levels.

This article focuses on modeling subnational migration patterns, which presents a particularly challenging test case for statistical demographic methods. Migration is widely recognized as a key driver of population change (Bijak 2010), yet it remains the most difficult of the three major demographic components to model. Unlike mortality and fertility, which follow relatively stable patterns, migration can exhibit high volatility, driven by economic shocks, policy changes, or conflicts, among others. This inherent complexity has motivated extensive research in Bayesian migration modeling (Bijak et al. 2008; Raymer et al. 2013; Azose & Raftery 2015; Wiśniowski et al. 2016; Zhang & Bryant 2020; Bijak 2024; Zens & Bijak 2025).

In particular, we consider the problem of modeling a comprehensive dataset on Austrian outmigration patterns, comprising district-specific outmigrant counts by single year of age ($x = 0, \dots, 95; A = 96$) and sex across 94 political districts from 2002 to 2023 ($T = 22$). The data, sourced from the Austrian national statistical office (*Statistik Austria*), are extracted from the central register of residents and define migration as any address change lasting longer than 90 days. The dataset combines internal and international outmigration and encompasses $N = 94 \times 2 = 188$ subpopulations defined by district–sex pairs. This period captures several major demographic disruptions that affected the Austrian migration system, including the 2015–2016 refugee crisis, the COVID-19 pandemic, and the Russian invasion of Ukraine in 2022. At the same time, district populations range from about 2 million residents in Vienna to fewer than 10,000 inhabitants in some rural areas, creating

heterogeneity both in demographic patterns and in the level of stochastic variation across populations.

Within this context, three specific modeling challenges emerge. First, small districts combined with single-year age groups produce numerous cells with 0–5 outmigrants, where stochastic variation can easily overwhelm genuine demographic signals. For small rural districts such as *Hermagor* (see Fig. 1), the raw age profiles fluctuate so strongly that year-to-year (and even age-to-age) changes are difficult to interpret and can even be misleading if taken at face value. Yet the data also exhibit clear regularities – such as peak migration between ages 20 and 30 – that effective models must capture. The first challenge thus lies in robustly separating genuine demographic patterns from random variation, while remaining flexible enough to capture regional and temporal heterogeneity. Statistical models face a difficult trade-off here, as aggressive smoothing loses important heterogeneity between regions, years, and age groups, while overly flexible models risk overfitting, particularly in sparse cells. Second, beyond denoising, modeling tools should ideally be able to extract meaningful patterns from the high-dimensional data and provide interpretable structural insights into the underlying processes, drivers, and shocks. This allows us to gain a deeper understanding of the demographic process of interest. Third, models must provide accurate forecasts for each age group and district, leveraging patterns across the entire dataset to improve predictions. This supports policy planning as well as population projection exercises. In granular demographic data, this quickly becomes a challenging, high-dimensional forecasting problem. For instance, the motivating dataset contains a total of $N \times A = 18,048$ individual time series. We will revisit and specifically focus on these three modeling challenges in the context of the real-world application in Sec. 5.

3 Related Literature and Research Gaps

3.1 Low-Rank Models in Statistical Demography

A family of models that has proven useful for partially overcoming the modeling challenges outlined in the previous section is based on low-rank approximation ideas, including SVDs and parametric factor models. Such models have been successfully applied in statistical demography for decades. Their success stems from the fact that demographic processes typically exhibit strong regularities across age and time. With respect to age, this is due to their direct link to biological processes (when considering fertility and mortality) and to life-course events (when considering migration). As a result, common patterns, such as increased mortality risk at older ages or peak migration activity between the ages of 20 and 30, can be efficiently extracted into a low-dimensional set of latent age factors. Similarly, demographic patterns often show strong co-movements across time, such as historically declining average mortality risk for all age groups or all subnational units under consideration. This common variation can be effectively summarized in a small number of latent underlying time factors.

For illustration, let $y_{i,t,x}$ denote a demographic count outcome of interest in population $i = 1, \dots, N$ (e.g., subnational units), time period $t = 1, \dots, T$, and age $x = 1, \dots, A$. The demographic counts are assumed to arise from conditionally independent Poisson distributions:

$$y_{i,t,x} \sim \mathcal{P}(e^{z_{i,t,x}}). \quad (1)$$

When modeling such multidimensional datasets, typical low-rank approximation modeling strategies tend to follow one of two conceptual approaches. First, from a time factorization point of view, the data can be decomposed using a structure similar to

$$z_{i,t,x} = \lambda'_{i,x} \mathbf{f}_t + \varepsilon_{i,t,x}, \quad \varepsilon_{i,t,x} \sim \mathcal{N}(0, \sigma^2). \quad (2)$$

In such models, the latent factors \mathbf{f}_t capture common variation over time, and the loadings $\lambda_{i,x}$ are estimated for each age and subpopulation. Examples of this perspective include the Lee–Carter model and its extensions (Lee & Carter 1992; Li & Lee 2005; Wiśniowski et al. 2015), among others. Dynamic latent factors \mathbf{f}_t are frequently considered as well (Czado et al. 2005). In the presence of three indices (i, t, x) , this approach requires estimation of the loadings $\lambda_{i,x}$ for each combination of subpopulation and age. This neglects the fact that the observed variation across ages x and subpopulations i typically follows certain regularities. Furthermore, when a large number of loadings must be estimated, both the risk of overfitting and the computational burden increase substantially.

Second, an age factorization perspective can be taken, where common age patterns are summarized in a small number of underlying age factors:

$$z_{i,t,x} = \lambda'_{i,t} \mathbf{f}_x + \varepsilon_{i,t,x}, \quad \varepsilon_{i,t,x} \sim \mathcal{N}(0, \sigma^2). \quad (3)$$

In this model, the latent factors \mathbf{f}_x capture common variation across ages, and the loadings $\lambda_{i,t}$ are estimated for each time period and subpopulation. Such approaches have been considered for instance in Alexander et al. (2017), Clark (2019), and Dharamshi et al. (2025). Domain knowledge, such as smoothness across ages in the latent factors \mathbf{f}_x , has been incorporated as well; see the Bayesian functional factor approach of Zens (2025). This perspective requires estimating the loadings $\lambda_{i,t}$ separately for each time t and subpopulation i , neglecting that these loadings may be highly correlated across time and subpopulations. Again, this quickly leads to computational and overfitting concerns.

Of course, in both cases, overfitting can be partially mitigated by considering additional structure on the loading elements, for example in the form of hierarchical or smoothing

priors. In fact, this is a common modeling strategy; see, for example, Alexander et al. (2017), Susmann et al. (2022), or Dharamshi et al. (2025). However, in settings with many subpopulations, estimating the loadings will still pose significant computational challenges in either factorization, irrespective of any hierarchical or smoothing structure. For example, considering an age factorization for the motivating dataset with $N = 188$ populations and $A = 96$ age groups measured over $T = 22$ years requires estimating more than 4,000 loadings $\lambda_{i,t}$ per time factor. A time factorization of the same dataset requires estimating more than 18,000 loadings $\lambda_{i,x}$ per age factor. Even in the presence of strong hierarchical prior information on the behavior of the loadings, this issue severely limits the scalability of existing demographic methods to high-dimensional data.¹

3.2 Statistical Approaches for Modeling Matrix and Tensor Data

While demographic applications have largely relied on single-margin factorizations, the statistical and machine learning literature offers a rich array of multi-way factorization methods that simultaneously exploit structure across multiple data dimensions. Hoff (2011b) considers array-normal models with separable covariance matrices. Hoff (2015) studies a multilinear tensor regression framework for relational data. Related matrix and tensor factor models are developed in Hoff (2011a). Shrinkage priors for regularization and automatic model selection are, for instance, discussed in Rai et al. (2014), Zhao et al. (2015), and Stolf & Canale (2025). More generally, Han et al. (2022) provides a unified treatment

¹Of course, many alternative approaches not based on low-rank approximations have been proposed for the analysis of demographic data over age and time, for example based on smoothing splines, functional data approaches, or log-linear models (Hyndman & Ullah 2007; Bryant & Zhang 2016; Camarda 2019; Pavone et al. 2024). In multi-population settings, overparameterization and computational issues also become significant challenges in these frameworks.

of low-rank tensor estimation (covering both Gaussian and Poisson likelihoods) with theoretical guarantees. Oseledets (2011) develop tensor-train factorizations enabling scalable representations of very high-order arrays.

A second strand of work develops dynamic matrix and tensor factor models, typically in Gaussian settings. Calder (2007) propose a bilinear latent factor structure for Gaussian observations, allowing for time dynamics and spatial smoothing. In macroeconometrics, Wang et al. (2019) consider a dynamic matrix factor model. Chen et al. (2022) extend this to tensor-valued observations. Billio et al. (2023) consider a dynamic Bayesian tensor regression model. Related dynamic matrix factor models with latent dynamic processes on the factors are studied by Yu et al. (2024), Qin et al. (2025), and Zhang (2024), who further allow for time-varying volatility, outlier adjustments, and flexible error covariances.

Closer to demography, a number of contributions exploit low-rank matrix or tensor structures. Russolillo et al. (2011) propose a Tucker-type decomposition of mortality surfaces over country, age, and year, assuming Gaussianity of log mortality rates and estimating the factors via SVD. Fosdick & Hoff (2014) develop a separable factor model for country–age–year mortality based on a separable probabilistic covariance model, conceptually related to separable space–time models popular in epidemiology and disease mapping (Martinez-Beneito et al. 2016).

For count data, available approaches range from classical nonnegative matrix factorization techniques (Lee & Seung 1999) to PARAFAC structures for tensors (Hu et al. 2015), hierarchical factorization approaches (Gopalan et al. 2015), and dynamic extensions (Charlin et al. 2015). The generalized estimation framework of Han et al. (2022) covers Poisson likelihoods as well. Schein et al. (2015) discuss a scalable Poisson tensor factorization model, combining conjugate gamma priors and variational inference for scalability.

3.3 Research Gaps and Contributions

Demographic factor models have successfully captured age and time patterns in population data, typically incorporating domain knowledge through smoothing priors and dynamic specifications. However, these models face a fundamental scalability challenge, as they typically factorize along a single margin, requiring loadings for every combination of the remaining dimensions. Even with hierarchical priors for information sharing, such parameterizations become computationally prohibitive and risk overfitting as the dimensionality of the data grows.

The statistical literature offers matrix and tensor factorization methods that could, in principle, solve this scalability problem through simultaneous factorization across multiple margins. Yet these methods are predominantly designed for Gaussian settings and typically do not incorporate the domain-specific constraints that make demographic models effective. The approaches that handle count data directly, such as Poisson tensor factorizations, typically lack the ability to incorporate prior knowledge such as smoothness across age, dynamic evolution over time, or the overdispersion needed to model sparse demographic data. This gap is particularly acute for small-population applications where many cells contain zero or near-zero counts. As a result, there is presently no framework that simultaneously leverages the parsimony of low-rank matrix factorizations and the structure of demographic processes in high-dimensional count data settings.

This paper bridges these streams of literature by developing a Bayesian matrix factor model that combines the computational efficiency of dual-margin factorization with the domain-specific structure of demographic modeling. We propose a bilinear factorization for matrix-valued count data that simultaneously decomposes the age and time margins through separate low-dimensional factors. This approach significantly reduces the num-

ber of parameters while incorporating demographic constraints through informative priors, providing smoothness across age and dynamic evolution for temporal factors. By working directly with overdispersed count likelihoods, the model naturally handles the sparse, heterogeneous data typical of subnational demographic applications. Working in the Bayesian paradigm further allows for fully probabilistic inference and coherent uncertainty quantification.

4 Matrix Factor Models for Age-Time Analysis

We consider modeling count-valued² observations $y_{i,t,x}$ measured in population i , at time point t , and at age x . The data are organized into N matrices of dimension $T \times A$, denoted as \mathbf{Y}_i , with elements $y_{i,t,x}$. The counts $y_{i,t,x}$ are assumed to arise from conditionally independent Poisson distributions,

$$y_{i,t,x} \sim \mathcal{P}(O_{i,t,x} e^{z_{i,t,x}}), \quad (4)$$

where $O_{i,t,x}$ is a fixed offset or exposure term representing, for example, an underlying known population size. We arrange the latent data $z_{i,t,x}$ in subpopulation-specific $T \times A$ matrices \mathbf{Z}_i and consider the following factorization for \mathbf{Z}_i :

$$\underbrace{\mathbf{Z}_i}_{T \times A} = \underbrace{\mathbf{F}_T}_{T \times Q} \underbrace{\mathbf{\Lambda}_i}_{Q \times R} \underbrace{\mathbf{F}'_A}_{R \times A} + \underbrace{\mathbf{E}_i}_{T \times A}. \quad (5)$$

In this representation, \mathbf{F}_T is a $T \times Q$ matrix with elements $f_{T,t,q}$, containing Q ($q = 1, \dots, Q$) potentially dynamic factors $\mathbf{f}_{T,q}$ of dimension $T \times 1$ that capture common variation across time (row dimension). \mathbf{F}_A is an $A \times R$ matrix with elements $f_{A,r,x}$, containing R ($r = 1, \dots, R$) potentially static factors $\mathbf{f}_{A,r}$ of dimension $A \times 1$ that capture common variation across age (column dimension).

²The considerations outlined in this article directly extend to Gaussian outcomes, as well as to binomial and negative binomial likelihood structures, which can be implemented via data augmentation approaches (Pillow & Scott 2012; Polson et al. 2013; Zens et al. 2024).

$r = 1, \dots, R$) factors $\mathbf{f}_{A,r}$ of dimension $A \times 1$ that capture common variation in the age dimension (column dimension).

The subpopulation-specific $Q \times R$ loading matrices $\mathbf{\Lambda}_i$ multiplicatively combine the information from the time and age factors to approximately recover the observed demographic process across age and time in subpopulation i . Each element of the error matrix \mathbf{E}_i , denoted as $\varepsilon_{i,t,x}$, is assumed to arise i.i.d. from $\mathcal{N}(0, \sigma_i^2)$, accounting for population-specific measurement error, stochastic variation, and overdispersion. This renders the model (4)–(5) effectively a Poisson lognormal bilinear factor model (Aitchison & Ho 1989). Beyond accounting for overdispersion, a major benefit of this setup is that, conditional on \mathbf{Z}_i , the model is Gaussian, which simplifies the structure of the conditional posterior densities significantly, even in complex settings with hierarchical priors that induce smoothing, time dynamics, or other complex dependency structures, as in Sec. 4.1. This flexibility comes at the price of an increased computational demand for posterior simulation, which typically requires data augmentation approaches (Tanner & Wong 1987). In comparison, conjugate Poisson–gamma setups as in Schein et al. (2015) are less computationally demanding, but make it more challenging to incorporate smoothing mechanisms or dynamic factor structures.

While similar in structure to an SVD, the bilinear representation (5) allows for non-diagonal $\mathbf{\Lambda}_i$, is based on sharing the matrices \mathbf{F}_T and \mathbf{F}_A across all populations i , and accounts for measurement error via \mathbf{E}_i . Thus, the factorization (5) can be most naturally interpreted as a Tucker-type decomposition, where the time and age modes of the time–age–population tensor are modeled using low-rank structure, while no compression is used for the population mode indexed by i . Related factorizations in Gaussian settings are discussed in the literature on modeling econometric and financial time series (Wang

et al. 2019; Zhang 2024; Yu et al. 2024), where observed matrices \mathbf{Z}_t are indexed by time, and the “sandwiched” matrices $\mathbf{\Lambda}_t$ are either modeled as unstructured or as following a matrix autoregressive model. In comparison, in factorization (5), time is a margin of the population-specific matrices \mathbf{Y}_i , and the matrices $\mathbf{\Lambda}_i$ are modeled independently from each other. This reflects the prior belief that, in demography, one may typically expect strong comovements across time and age patterns, but not necessarily across (sub-)populations i indexing sex, geographical units, or other stratifications that may be highly heterogeneous in terms of how they combine the information in the shared age and time factors.

It is further illustrative to compare the factorization in (5) with the age and time factorization perspectives discussed in Sec. 3. From an age factorization perspective, (5) can be rewritten as

$$\underbrace{\mathbf{Z}_i}_{T \times A} = \underbrace{\mathbf{\Lambda}_i^*}_{T \times R} \underbrace{\mathbf{F}'_A}_{R \times A} + \underbrace{\mathbf{E}_i}_{T \times A}, \quad (6)$$

where factors are extracted in the age dimension, and the subpopulation–time-specific loadings $\mathbf{\Lambda}_i^* = \mathbf{F}_T \mathbf{\Lambda}_i$ use common factors across time to reduce the dimensionality of the loading matrix. Similarly, from a time factorization perspective, (5) can be rewritten as

$$\underbrace{\mathbf{Z}_i}_{T \times A} = \underbrace{\mathbf{F}_T}_{T \times Q} \underbrace{\mathbf{\Lambda}_i^*}_{Q \times A} + \underbrace{\mathbf{E}_i}_{T \times A}, \quad (7)$$

where factors are extracted in the time dimension, and the subpopulation–age-specific loadings $\mathbf{\Lambda}_i^* = \mathbf{\Lambda}_i \mathbf{F}'_A$ use common factors across age to reduce the dimensionality of the loading matrix.

The proposed factorization extracts relevant common variation across both age and time into two sets of low-dimensional factors, leading to a parsimonious representation of the data at hand. The number of population-specific parameters ($\mathbf{\Lambda}_i, \sigma_i^2$) can potentially be reduced significantly compared to single-margin factorizations, from $NQA + N$ (time factorization) and $NRT + N$ (age factorization) to $NQR + N$. In the motivating application in Sec. 5, we

use $Q = 6$ and $R = 8$. Given $N = 188$ populations, $A = 96$ age groups, and $T = 22$ years, the proposed matrix factor model thus requires estimation of 9,212 population-specific parameters in total. In this example, the number of parameters is reduced to about 27.7% of the number of parameters in an age factorization model with $R = 8$ (33,276 parameters), and to about 8.5% of the number of parameters in a time factorization model with $Q = 6$ (108,476 parameters).

4.1 Prior Specification

The Bayesian paradigm enables the elicitation of suitable prior distributions on all parameters. For the latent factors, we use informative, structural priors that reflect domain knowledge. First, to allow for time dynamics and facilitate forecasting, we assume the time factors $f_{T,t,q}$ evolve over time according to a first-order random walk with drift,

$$f_{T,t,q} = \kappa_q + f_{T,t-1,q} + \eta_{T,t,q}, \quad \eta_{T,t,q} \sim \mathcal{N}(0, \tau_{T,q}). \quad (8)$$

This choice allows the model to capture potentially complex and nonstationary trends. Random-walk-with-drift dynamics with expanding uncertainty bands are a natural choice here, especially when modeling potentially volatile and hard-to-predict migration dynamics (Bijak 2010). Similar specifications are also widely used in mortality modeling (Lee & Carter 1992).

Based on demographic theory and empirical evidence, accounting for smoothness in the age dimension is also typically desirable (Camarda 2012; Hyndman et al. 2013; Pavone et al. 2024). This is motivated by the fact that demographic outcomes of neighboring age groups are typically relatively similar. We utilize this prior knowledge by assuming that the age factors $\mathbf{f}_{A,r} = (f_{A,r,1}, \dots, f_{A,r,A})'$ follow an intrinsic conditional autoregressive (ICAR) prior on the one-dimensional age graph. The implied full conditional distribution of $f_{A,r,x}$

is

$$f_{A,r,x} \mid \mathbf{f}_{A,r,-x}, \tau_{A,r} \sim \mathcal{N}\left(\frac{1}{n_x} \sum_{x' \sim x} f_{A,r,x'}, \frac{\tau_{A,r}}{n_x}\right), \quad (9)$$

where the sum is over the neighboring ages $x' \sim x$ and where n_x denotes the number of neighboring ages for age x ($n_x = 2$ for interior ages and $n_x = 1$ at the boundaries).

Alternative prior structures for the columns of \mathbf{F}_A can easily be incorporated by assuming, for example, adaptive smoothing priors (Lang & Brezger 2004), or by assuming that the factors can be well represented using smooth B-spline expansions (Zens 2025) or Gaussian processes. Similarly, for the columns of \mathbf{F}_T , more restrictive (e.g., second-order random walk) or more complex (e.g., dependent autoregressive systems) state dynamics over time could be incorporated. An interesting extension of the framework could include an explicit model selection mechanism (e.g., based on shrinkage priors or model averaging techniques) in the equations governing the dynamics of the columns of \mathbf{F}_T and \mathbf{F}_A .

We choose the remaining priors to be at most weakly informative. Jeffreys priors $p(\tau_{T,q}) \propto \tau_{T,q}^{-1}$ and $p(\tau_{A,r}) \propto \tau_{A,r}^{-1}$ are specified on the state variance parameters. We use flat priors $p(\kappa_q) \propto 1$ and $p(f_{T,0,q}) \propto 1$ on the drift parameters and initial values of the time factors. For the latent error variances, we use $\sigma_i^2 \sim \mathcal{IG}(c_0, C_0)$ and set $c_0 = 2.5$ and $C_0 = 1.5$. For the loading parameters $\mathbf{\Lambda}_i$, we assume elementwise Gaussian priors $\lambda_{i,q,r} \sim \mathcal{N}(0, L_{0,i,q,r})$. We denote the implied multivariate Gaussian prior on $\text{vec}(\mathbf{\Lambda}_i)$ as $\text{vec}(\mathbf{\Lambda}_i) \sim \mathcal{N}(0, \mathbf{L}_{0,i})$, where $\mathbf{L}_{0,i}$ is a diagonal matrix with appropriately ordered diagonal elements $L_{0,i,q,r}$. By default, $L_{0,i,q,r} = 1$ is used in the illustrations below. Extensions and useful alternatives to the proposed prior framework are discussed in Sec. 6.

Finally, we treat the number of factors, Q and R , as fixed prior choices made by the researcher. Selecting an appropriate number of factors in latent factor models for matrices and tensors is, in general, a nontrivial statistical problem (Lopes & West 2004). The

literature proposes a range of approaches: from heuristics based on scree plots, classical model selection criteria, and marginal likelihood estimates, to automatic model selection using shrinkage priors (Rai et al. 2014; Zhao et al. 2015; Stolf & Canale 2025), mixing over the number of factors during MCMC (Frühwirth-Schnatter et al. 2024), and model selection based on predictive measures from pseudo-out-of-sample evaluations. In this article, we adopt the latter approach, employing extensive cross-validation and out-of-sample forecasting exercises – described in detail in Sec. 5 – to select appropriate values for Q and R .

4.2 Parameter Estimation

The proposed posterior simulation scheme for parameter estimation relies on the fact that, conditional on \mathbf{Z}_i , the remaining model is a Gaussian bilinear factor model, offering closed-form conditional posteriors for all parameters of interest. This makes data augmentation, where the algorithm iterates between (i) imputing the latent \mathbf{Z}_i conditional on the remaining parameters and (ii) updating the remaining parameters conditional on \mathbf{Z}_i , a natural candidate for posterior simulation (Tanner & Wong 1987). To update $z_{i,t,x}$, we use univariate adaptive Metropolis updates in the style of Roberts & Rosenthal (2009). Gradient-based updates have also been proposed for this step (Steel & Zens 2024), but are typically more complex to implement and have relatively high computational cost when considering large numbers of latent observations, which partially offsets their efficiency gains. In the interest of brevity, full MCMC details are given in the supplementary materials (Sec. S1), together with a simulation exercise (Sec. S2).

Two observations are worth highlighting. First, if \mathbf{Z}_i is observed – as, for example, in Gaussian data settings – the proposed MCMC algorithm directly applies. Similarly,

if \mathbf{Z}_i is a latent outcome in data augmentation schemes for binary or categorical data (Zens et al. 2024), the algorithm extends directly as well. Second, it is important to note that latent factorizations such as (5) suffer from several sources of identification issues, including rotational and scale indeterminacy, sign switching, and column switching (Conti et al. 2014; Frühwirth-Schnatter et al. 2024). Regarding scaling, the standard normal priors on the elements of $\mathbf{\Lambda}_i$ aid identification. Regarding rotation and ordering invariance, proposed solutions include the introduction of loading restrictions (Lopes & West 2004), orthonormality restrictions during MCMC (Kowal & Bourgeois 2020), priors that enforce orthogonality (Jauch et al. 2021), and ex-post identification schemes (Aßmann et al. 2016; Frühwirth-Schnatter et al. 2024). In the proposed MCMC routine, we leave the loadings unrestricted and allow the Markov chain to freely explore rotations and orderings. We resort to simple exploratory post-processing steps when discussing the broad patterns captured by the factors \mathbf{F}_A and \mathbf{F}_T in Sec. 5.

5 Application to Austrian Migration Data

The proposed posterior simulation algorithm is used to collect 25,000 posterior samples after an initial burn-in period of 7,500 iterations. We set $O_{i,t,x} = 1$ for all data cells and focus on modeling the outmigration counts directly. MCMC convergence behavior is generally satisfactory. Example trace plots for identified parameters are provided in the supplementary materials (Fig. S4).

For model selection, we perform a ten-fold cross-validation exercise in which we repeatedly predict randomly partitioned 10% hold-out samples after training models on the remaining 90% of the data. We consider 100 possible models resulting from combining $Q \in \{1, \dots, 10\}$ and $R \in \{1, \dots, 10\}$. For evaluation, we collect log predictive scores

(LPS), root mean squared errors (RMSEs), mean absolute errors (MAEs), and correlations of the log-transformed true values relative to the posterior means of the log-transformed posterior predictive distribution of the counts $y_{i,t,x}$. In general, various combinations of Q and R give very similar results, and the objective surface is relatively flat along those trade-off directions. Results for $Q = 6$ and $R = 8$ latent factors are presented in detail below, as this setting provides a good balance between model fit and complexity. In our application, this setting is typically among the most parsimonious specifications within one standard error of the best-performing model for each considered criterion. Detailed results for all settings and criteria are given in the supplementary materials (Fig. S5).

We now revisit the three main modeling challenges described in Sec. 2, namely the ability to effectively denoise and smooth the observed data, the ability to provide interpretable structural insights into the data-generating process, and the ability to provide accurate forecasts.

Denoising. Regarding denoising performance in tracking historical demographic trends and patterns, Fig. 2 presents observed data alongside fitted values for a small (bottom) and a medium-sized (top) subpopulation. The left pair of columns shows the data in the form of classical age curves, while the right pair of columns provides a bird’s-eye view of the annual age patterns. The results clearly show how the model can smooth out stochastic noise in smaller subpopulations by borrowing information about demographic patterns from other subpopulations, while more closely following the patterns observed in more informative subpopulations.

From a substantive perspective, this type of model-based denoising is directly relevant for regional policy analysis. For small rural districts (Fig. 2, bottom panels), the raw age profiles are noisy, making direct interpretation difficult and potentially misleading. The

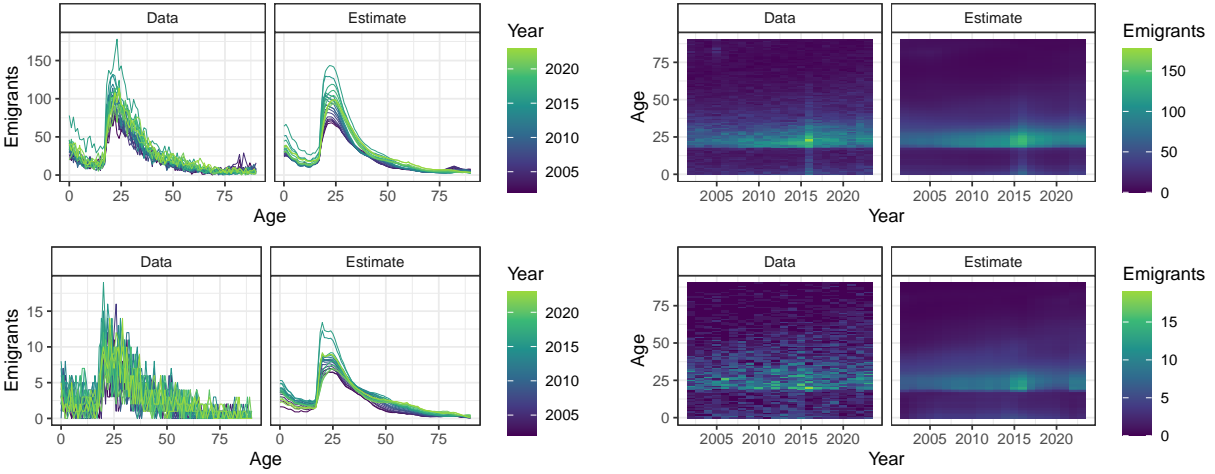


Figure 2: Observed and fitted outmigration counts for two subpopulations. The top row shows data for females migrating from a district with a medium-sized population and relatively low noise level. The bottom row shows data for males migrating from a sparsely populated rural area with significant stochastic variation in the raw data. Pairs of plots in the left and right columns show the same data and estimates from different perspectives. Fitted values are posterior means of the respective posterior predictive densities.

matrix factor model delivers smooth, age-specific migration schedules that still preserve genuine local particularities. Crucially, while the model smooths out noise, it does not oversmooth years corresponding to shock events (such as the 2015–2016 refugee inflows), and it preserves certain non-smooth age patterns (such as spikes at ages 18 and 19, where many young people migrate for education or for mandatory military service) that provide insights into the underlying demographic process. The model-based estimates can even reveal subtle patterns such as increasing retirement outmigration between ages 50 and 75 in the most recent years. For practitioners, this combination of robustness and flexibility provides a much more stable basis for applications such as school planning, housing demand assessment, or the design of local labor market programs.

Structural insights. To gain structural insights into broad patterns across time and age, we apply a simple tensor decomposition to the posterior mean of the fitted values $\mathbf{F}_T \mathbf{\Lambda}_i \mathbf{F}'_A$. Specifically, we first remove the population-specific mean levels from the fitted $T \times A \times N$ array so that the subsequent components describe deviations in shape rather than just average differences in levels. We then perform a singular value decomposition on the age and time modes of this centered array, which yields orthogonal time and age components ordered by their contribution to the variation in the fitted surfaces.

Supplementary Fig. S3 shows the extracted factors in the age and time dimensions. The age factors modulate the behavior of the subpopulation-specific data at specific ages and follow intuitive patterns. For example, the first factor clearly resembles a sign-flipped log-transformed Rogers–Castro model migration schedule, which is a well-known parametric migration schedule reflecting regularities in migration patterns over the life course (Rogers et al. 1978). Notably, the model recovers this familiar life-course pattern of educational and early career migration without imposing it a priori. The remaining factors mainly modulate behavior at specific ages, such as around ages 18–20 (when young adults typically move for education or military service) or between ages 75 and 95 (where increased mobility patterns indicate that people are moving into retirement homes).

The time factors reveal similarly interpretable structure, capturing long-run demographic developments in the form of approximately linear (Factor 2) and quadratic (Factor 3) trends, as well as distinct dynamics that disrupted the Austrian migration system. Specifically, the factors recover significant spikes in migration activity, driven primarily by conflict-induced migration from the Middle East (in 2015 and 2016) and from Ukraine (in 2022). In both cases, large international migration inflows led to subsequent internal migration movements, which are reflected in the estimated factors. Similarly, the onset of

the COVID-19 pandemic in 2020 is clearly captured in the factors (e.g., Factors 5 and 6).

Taken together, the age and time factors provide a directly inspectable, low-dimensional representation of complex demographic patterns, condensing thousands of demographic series into a handful of components. This illuminates which parts of the age profile and which periods in time account for most of the variation in multidimensional demographic processes. For practitioners, this decomposition offers a structured way to explore past and recent demographic developments, focusing attention on the dominant life-course patterns and temporal shocks that drive observed changes.

While these components provide a convenient summary of the main patterns captured by the model, it is crucial to recognize that this ex-post SVD approach represents only one particular orthonormal basis for the space spanned by the factors, chosen for its convenient ordering by explained variation. Any rotation of these factors would be equally valid from an identification perspective, and thus an overly strong direct causal interpretation of individual estimated factors should be avoided. Nevertheless, the subspace spanned by these factors does capture meaningful structural patterns in the data, allowing us to identify and characterize the dominant modes of variation across time and age.

Forecasting and predictive exercise. We now turn to the third modeling challenge outlined in Sec. 2, namely forecasting. The modeling framework can be used to obtain probabilistic forecasts for the counts $y_{i,t,x}$. Conveniently, obtaining these high-dimensional forecasts requires only forecasting the Q dynamic factors in \mathbf{F}_T , which are the only time-varying components in the proposed matrix factor model. This renders the forecasting problem a relatively low-dimensional statistical exercise. In practical terms, this allows analysts to produce coherent demographic forecasts for hundreds or thousands of populations simultaneously through a computationally tractable approach.

Given the first-order random walk dynamics, forecasts can be obtained by iterating $f_{T,t,q} = \kappa_q + f_{T,t-1,q} + \eta_{T,t,q}$ forward in time for each q . Monte Carlo simulation then makes it possible to obtain a full posterior distribution of forecasts for the Q factors. Combining these with the static loadings $\mathbf{\Lambda}_i$ and the age factors \mathbf{F}_A then allows us to obtain forecasts for the elements of \mathbf{Z}_i and, consequently, for the counts \mathbf{Y}_i .³ This recovers full probabilistic forecasts for all age–sex–subpopulation-specific time series. Importantly, Monte Carlo simulation also allows us to obtain the posterior distribution of functionals of these forecasts, if of interest. For example, predicted migration patterns for individuals aged 15 to 20 can be aggregated, which may serve as an index to track and project the attractiveness of districts for younger populations.

To assess the usefulness of the model for forecasting demographic patterns, we implement a predictive exercise. We use a moving-window setting with a training period of 17 years. The last five observed years (2019–2023) are used as hold-out samples to evaluate pseudo-out-of-sample predictions. In the first hold-out period, we generate forecasts for $t+1$ (2019) and $t+5$ (2023) to evaluate the short- and medium-term accuracy of the predictions. For the remaining four forecast windows, we collect forecasts for $t+1$ (2020–2023).

We compare the Bayesian matrix factor model to six alternative modeling frameworks. We consider independent random walks, with and without drifts, as simple benchmarks. In addition, four SVD-based factorizations of the log-transformed counts, similar to the models outlined in Sec. 3.1, are considered. First, we extract factors in the time dimension and forecast these time-varying factors as random walks with drifts. Second, we extract factors in the age dimension and forecast the time-varying loadings, specified as random walks with drifts. Both SVD-based models are estimated once separately for each subpop-

³For example, if $\mathbf{f}_{T,t+h}$ denotes the $1 \times Q$ row vector of factor forecasts for $t+h$, then $\mathbf{f}_{T,t+h}\mathbf{\Lambda}_i\mathbf{F}'_A$ gives the forecasts $z_{i,t+h,x}$ for individual i , and $y_{i,t+h,x}$ can be simulated from $y_{i,t+h,x} \sim \mathcal{P}(e^{z_{i,t+h,x}})$.

Table 1: Forecast performance at one-year and five-year horizons

Model	One-year horizon					Five-year horizon				
	Q	R	RMSE	MAE	Corr.	Q	R	RMSE	MAE	Corr.
Random Walk	-	-	0.526	0.384	0.907	-	-	0.564	0.415	0.901
Random Walk w. Drift	-	-	0.542	0.399	0.901	-	-	0.649	0.482	0.873
Time Factorization	1	1	0.437	0.332	0.936	1	1	0.475	0.364	0.930
Joint Time Factorization	1	1	0.433	0.328	0.936	2	1	0.474	0.361	0.928
Age Factorization	1	1	0.448	0.355	0.939	1	1	0.520	0.415	0.933
Joint Age Factorization	1	4	0.439	0.348	0.942	1	2	0.508	0.403	0.937
Bayesian Matrix Factorization	2	6	0.405	0.305	0.944	2	4	0.418	0.321	0.940

Notes: RMSE = Root Mean Squared Error, MAE = Mean Absolute Error, Corr. = Correlation Coefficient. For comparability, results are presented on the log-count scale and averaged across all ages, holdout periods, and subpopulations. Column-wise best performance is highlighted in **bold**. Selected Q and R values are based on the best performance in terms of RMSE.

ulation i to allow for more flexibility, and once in an alternative setting where the factors are approximated jointly across all subpopulations to borrow more strength. Where applicable, the number of extracted latent factors is varied between 1 and 10 (considering all 100 combinations for the Bayesian framework). More details on competitor models and their implementation are given in the supplementary materials (Sec. S3). To evaluate the predictions, we collect RMSEs, MAEs, and correlations of the true values relative to the point predictions for the log-transformed counts. For the Bayesian model, this corresponds to the posterior means of the log-transformed posterior predictive density of $y_{i,t,x}$.

The results of this exercise are provided in Tab. 1. The Bayesian matrix factor model outperforms all other models on all predictive measures evaluated, underlining its potential for demographic modeling and projection exercises. The naïve random walk with drift typically performs worst, reflecting that unrestricted linear trends for all population–age-specific time series clearly overfit the noisy data. The results also suggest that using a joint

single-margin factorization approach that borrows strength across populations outperforms factorizations estimated separately for each population.

Relative to a simple random walk benchmark on the log scale, the proposed model reduces one-year-ahead RMSE by about 23% (from 0.526 to 0.405) and five-year-ahead RMSE by about 26% (from 0.564 to 0.418). Even when compared to the best-performing single-margin factorization, the matrix factor model achieves around 6.5% lower RMSE at the one-year horizon (0.433 vs. 0.405) and roughly 12% lower RMSE at the five-year horizon (0.474 vs. 0.418). Thus, the significant gains in parsimony do not come at the expense of forecast accuracy – if anything, they yield more reliable short- and medium-term projections.

Note that this exercise does not imply either that the predictive performance of the Bayesian matrix model in its current form exhibits some sort of ‘optimality’ in all conceivable settings, or that it outperforms all alternative dynamic matrix and tensor factorization frameworks. Rather, it indicates a certain degree of predictive robustness and no reduction in the predictive performance of the Bayesian model despite its much more parsimonious nature. An important real-world implication of this exercise is that higher-order decompositions of demographic processes can offer significant predictive advantages over more heavily parameterized single-margin approaches. Several ways to further optimize predictive power for demographic applications and beyond are discussed in the next section.

6 Discussion and Concluding Remarks

In this article, we propose a Bayesian matrix factor model for count data, focusing on applications to demographic data recorded by age, time, and population. The model is introduced with an informative prior setting, and a simple MCMC estimation algorithm is

developed for posterior simulation. The framework is applied to a challenging real-world dataset, and a pseudo-out-of-sample prediction exercise is conducted.

The results suggest that the model effectively addresses three intertwined modeling challenges in the field: the denoising of small counts with highly complex dependency structures, the provision of interpretable structural insights into the underlying demographic process, and the accurate forecasting of a large number of individual time series. These results underscore its potential for applications in statistical demography and related fields dealing with non-Gaussian, noisy, and heterogeneous matrix-valued data.

Several avenues for future research emerge. First, we see our findings as a baseline for further investigations of structured probabilistic tensor factorizations for demographic applications. For statistical offices or planning agencies, such advances may provide frameworks that can be scaled to larger systems (e.g., more districts or additional stratifications) while keeping the number of parameters to be estimated manageable. Future research may extend the presented methodology to higher-order tensors using full Tucker or tensor-train (Oseledets 2011) decompositions, potentially leading to scalable modeling tools when data are stratified by many demographic dimensions.

In terms of demographic applications, this article focuses on migration data, typically the most challenging of the three demographic components to model and predict. Model evaluations in the context of mortality and fertility data will provide further insight into model performance. We anticipate the model to perform at least as well in these applications, as mortality and fertility patterns are typically more regular over age and time than migration patterns, which plays to the strengths of low-rank factorization methods.

In terms of prior and model setup, hierarchical priors on the factor loadings that enhance information sharing between subpopulations are likely to further improve predictive

power (Alexander et al. 2017; Clark 2019; Zens 2025; Dharamshi et al. 2025). Similarly, shrinkage priors (Legramanti et al. 2020; Stolf & Canale 2025) could be used to regularize the factor loadings, increase robustness against overfitting, aid model selection, and reflect the prior belief that not all factors (and their interactions) are expected to be relevant for every subpopulation. The inclusion of covariates measured by age, subpopulation, and/or time point, in addition to the latent factors, could potentially further improve model performance. More flexible error variance structures are relatively straightforward extensions as well, but lead to slightly more complex MCMC schemes.

In terms of estimation, this article considers a Bayesian approach based on MCMC sampling that allows for exact posterior inference. The trade-off is that MCMC methods come at a relatively high computational cost. Two computationally cheaper alternatives could be explored. First, approximate maximum likelihood estimates can be obtained in a two-step process. In the first step, the factor matrices \mathbf{F}_T and \mathbf{F}_A could be extracted from log-transformed demographic counts and rates based on tensor generalizations of singular value decompositions (De Lathauwer et al. 2000). In the second step, the loading matrices $\mathbf{\Lambda}_i$ are estimated by ordinary least squares independently for each subpopulation i . This approach is a potentially crude approximation to the true posterior but comes at a much lower computational cost and may therefore be attractive to practitioners. If forecasting is required, a third step can be added in which time series models for the Q time factors in \mathbf{F}_T are fitted ex post and used for forecasting. Such multi-step procedures are in line with current practice in applied demographic research (Lee & Carter 1992; Alexander et al. 2017) and have been used to obtain the initial values for the MCMC algorithm in the present article. As a second alternative, closer to the Bayesian paradigm, variational Bayes (VB) algorithms could be developed to approximate the posterior densities of interest,

combining ideas from VB for factor analysis (Hansen et al. 2024) and VB for Poisson lognormal frameworks (Chiquet et al. 2019).

Many of the pathways discussed above share the common overarching goal of effectively scaling statistical models in multidimensional demographic research to higher-order, multi-indexed data. This challenge is particularly evident in migration modeling, where data are often cross-tabulated by origin, destination, age, sex, time, and possibly additional dimensions such as education or citizenship. In very high-dimensional settings, several computational and model-related challenges remain and require further advances in the computational and theoretical foundations of statistical demography.

Data Availability Statement

The data that support the findings of this study are openly available in the public data repository *StatCube* of *Statistik Austria* at <https://www.statistik.at/en/databases/statcube-statistical-database> (*Wanderungsstatistik*).

References

- Aitchison, J. & Ho, C. (1989), ‘The multivariate Poisson-log normal distribution’, *Biometrika* **76**(4), 643–653.
- Alexander, M., Zagheni, E. & Barbieri, M. (2017), ‘A flexible Bayesian model for estimating subnational mortality’, *Demography* **54**(6), 2025–2041.
- Aßmann, C., Boysen-Hogrefe, J. & Pape, M. (2016), ‘Bayesian analysis of static and dynamic factor models: An ex-post approach towards the rotation problem’, *Journal of Econometrics* **192**(1), 190–206.

- Azose, J. J. & Raftery, A. E. (2015), ‘Bayesian probabilistic projection of international migration’, *Demography* **52**(5), 1627–1650.
- Bijak, J. (2010), *Forecasting international migration in Europe: A Bayesian view*, Vol. 24, Springer Science & Business Media.
- Bijak, J. (2024), *From Uncertainty to Policy: A Guide to Migration Scenarios*, Edward Elgar Publishing.
- Bijak, J., Raymer, J. & Willekens, F. (2008), ‘Bayesian methods in international migration forecasting’, *International migration in Europe: Data, models and estimates* pp. 255–288.
- Billio, M., Casarin, R., Iacopini, M. & Kaufmann, S. (2023), ‘Bayesian dynamic tensor regression’, *Journal of Business & Economic Statistics* **41**(2), 429–439.
- Bryant, J. & Zhang, J. L. (2016), ‘Bayesian forecasting of demographic rates for small areas: emigration rates by age, sex, and region in New Zealand, 2014-2038’, *Statistica Sinica* pp. 1337–1363.
- Calder, C. A. (2007), ‘Dynamic factor process convolution models for multivariate space–time data with application to air quality assessment’, *Environmental and Ecological Statistics* **14**(3), 229–247.
- Camarda, C. G. (2012), ‘MortalitySmooth: An R package for smoothing Poisson counts with P-splines’, *Journal of Statistical Software* **50**, 1–24.
- Camarda, C. G. (2019), ‘Smooth constrained mortality forecasting’, *Demographic Research* **41**, 1091–1130.

- Charlin, L., Ranganath, R., McInerney, J. & Blei, D. M. (2015), Dynamic Poisson factorization, *in* ‘Proceedings of the 9th ACM Conference on Recommender Systems’, pp. 155–162.
- Chen, R., Yang, D. & Zhang, C.-H. (2022), ‘Factor models for high-dimensional tensor time series’, *Journal of the American Statistical Association* **117**(537), 94–116.
- Chiquet, J., Robin, S. & Mariadassou, M. (2019), Variational inference for sparse network reconstruction from count data, *in* ‘International Conference on Machine Learning’, PMLR, pp. 1162–1171.
- Clark, S. J. (2019), ‘A general age-specific mortality model with an example indexed by child mortality or both child and adult mortality’, *Demography* **56**(3), 1131–1159.
- Conti, G., Frühwirth-Schnatter, S., Heckman, J. J. & Piatek, R. (2014), ‘Bayesian exploratory factor analysis’, *Journal of Econometrics* **183**(1), 31–57.
- Czado, C., Delwarde, A. & Denuit, M. (2005), ‘Bayesian Poisson log-bilinear mortality projections’, *Insurance: Mathematics and Economics* **36**(3), 260–284.
- De Lathauwer, L., De Moor, B. & Vandewalle, J. (2000), ‘A multilinear singular value decomposition’, *SIAM journal on Matrix Analysis and Applications* **21**(4), 1253–1278.
- Dharamshi, A., Alexander, M., Winant, C. & Barbieri, M. (2025), ‘Jointly estimating subnational mortality for multiple populations’, *Demographic Research* **52**, 71–110.
- Fosdick, B. K. & Hoff, P. D. (2014), ‘Separable factor analysis with applications to mortality data’, *The Annals of Applied Statistics* **8**(1), 120.
- Frühwirth-Schnatter, S., Hosszejni, D. & Lopes, H. F. (2024), ‘Sparse Bayesian factor analysis when the number of factors is unknown’, *Bayesian Analysis* **1**(1), 1–31.

- Gopalan, P., Hofman, J. M. & Blei, D. M. (2015), Scalable recommendation with hierarchical Poisson factorization, *in* ‘Proceedings of the Thirty-First Conference on Uncertainty in Artificial Intelligence’, pp. 326–335.
- Han, R., Willett, R. & Zhang, A. R. (2022), ‘An optimal statistical and computational framework for generalized tensor estimation’, *The Annals of Statistics* **50**(1), 1–29.
- Hansen, B., Avalos-Pacheco, A., Russo, M. & De Vito, R. (2024), ‘Fast variational inference for Bayesian factor analysis in single and multi-study settings’, *Journal of Computational and Graphical Statistics* (just-accepted), 1–42.
- Hoff, P. D. (2011a), ‘Hierarchical multilinear models for multiway data’, *Computational Statistics & Data Analysis* **55**(1), 530–543.
- Hoff, P. D. (2011b), ‘Separable covariance arrays via the Tucker product, with applications to multivariate relational data’, *Bayesian Analysis* **6**(2), 179–196.
- Hoff, P. D. (2015), ‘Multilinear tensor regression for longitudinal relational data’, *The Annals of Applied Statistics* **9**(3), 1169.
- Hu, C., Rai, P., Chen, C., Harding, M. & Carin, L. (2015), Scalable Bayesian non-negative tensor factorization for massive count data, *in* ‘Joint European Conference on Machine Learning and Knowledge Discovery in Databases’, Springer, pp. 53–70.
- Hyndman, R. J., Booth, H. & Yasmeen, F. (2013), ‘Coherent mortality forecasting: the product-ratio method with functional time series models’, *Demography* **50**(1), 261–283.
- Hyndman, R. J. & Ullah, M. S. (2007), ‘Robust forecasting of mortality and fertility rates: A functional data approach’, *Computational Statistics & Data Analysis* **51**(10), 4942–4956.

- Jauch, M., Hoff, P. D. & Dunson, D. B. (2021), ‘Monte Carlo simulation on the Stiefel manifold via polar expansion’, *Journal of Computational and Graphical Statistics* **30**(3), 622–631.
- Kowal, D. R. & Bourgeois, D. C. (2020), ‘Bayesian function-on-scalars regression for high-dimensional data’, *Journal of Computational and Graphical Statistics* **29**(3), 629–638.
- Lang, S. & Brezger, A. (2004), ‘Bayesian P-splines’, *Journal of Computational and Graphical Statistics* **13**(1), 183–212.
- Lee, D. D. & Seung, H. S. (1999), ‘Learning the parts of objects by non-negative matrix factorization’, *nature* **401**(6755), 788–791.
- Lee, R. D. & Carter, L. R. (1992), ‘Modeling and forecasting US mortality’, *Journal of the American statistical association* **87**(419), 659–671.
- Legramanti, S., Durante, D. & Dunson, D. B. (2020), ‘Bayesian cumulative shrinkage for infinite factorizations’, *Biometrika* **107**(3), 745–752.
- Li, N. & Lee, R. (2005), ‘Coherent mortality forecasts for a group of populations: An extension of the Lee-Carter method’, *Demography* **42**, 575–594.
- Lopes, H. F. & West, M. (2004), ‘Bayesian model assessment in factor analysis’, *Statistica Sinica* pp. 41–67.
- Martinez-Beneito, M. A., Botella-Rocamora, P. & Banerjee, S. (2016), ‘Towards a multidimensional approach to Bayesian disease mapping’, *Bayesian analysis* **12**(1), 239.
- Oseledets, I. V. (2011), ‘Tensor-train decomposition’, *SIAM Journal on Scientific Computing* **33**(5), 2295–2317.

- Pavone, F., Legramanti, S. & Durante, D. (2024), ‘Learning and forecasting of age-specific period mortality via B-spline processes with locally-adaptive dynamic coefficients’, *The Annals of Applied Statistics* **18**(3), 1965–1987.
- Pillow, J. & Scott, J. (2012), ‘Fully Bayesian inference for neural models with negative-binomial spiking’, *Advances in neural information processing systems* **25**, 1898–1906.
- Polson, N. G., Scott, J. G. & Windle, J. (2013), ‘Bayesian inference for logistic models using Pólya–Gamma latent variables’, *Journal of the American statistical Association* **108**(504), 1339–1349.
- Qin, L., Wang, Y., Zhu, Y. & Shia, B.-C. (2025), ‘Bayesian Dynamic Matrix Factor Models’, *Journal of Business & Economic Statistics* pp. 1–13.
- Rai, P., Wang, Y., Guo, S., Chen, G., Dunson, D. & Carin, L. (2014), Scalable Bayesian low-rank decomposition of incomplete multiway tensors, *in* ‘International conference on machine learning’, PMLR, pp. 1800–1808.
- Raymer, J., Wiśniowski, A., Forster, J. J., Smith, P. W. & Bijak, J. (2013), ‘Integrated modeling of European migration’, *Journal of the American Statistical Association* **108**(503), 801–819.
- Roberts, G. O. & Rosenthal, J. S. (2009), ‘Examples of adaptive MCMC’, *Journal of computational and graphical statistics* **18**(2), 349–367.
- Rogers, A., Raquillet, R. & Castro, L. J. (1978), ‘Model migration schedules and their applications’, *Environment and Planning A* **10**(5), 475–502.
- Rue, H. & Held, L. (2005), *Gaussian Markov random fields: theory and applications*, Chapman and Hall/CRC.

- Russolillo, M., Giordano, G. & Haberman, S. (2011), ‘Extending the Lee–Carter model: a three-way decomposition’, *Scandinavian Actuarial Journal* **2011**(2), 96–117.
- Schein, A., Paisley, J., Blei, D. M. & Wallach, H. (2015), Bayesian Poisson tensor factorization for inferring multilateral relations from sparse dyadic event counts, *in* ‘Proceedings of the 21th ACM SIGKDD International conference on knowledge discovery and data mining’, pp. 1045–1054.
- Steel, M. & Zens, G. (2024), ‘Model Uncertainty in Latent Gaussian Models with Univariate Link Function’, *arXiv preprint arXiv:2406.17318* .
- Stolf, F. & Canale, A. (2025), ‘Bayesian Adaptive Tucker Decompositions for Tensor Factorization’, *Journal of Computational and Graphical Statistics* (just-accepted), 1–18.
- Susmann, H., Alexander, M. & Alkema, L. (2022), ‘Temporal Models for Demographic and Global Health Outcomes in Multiple Populations: Introducing a New Framework to Review and Standardise Documentation of Model Assumptions and Facilitate Model Comparison’, *International Statistical Review* **90**(3), 437–467.
- Tanner, M. A. & Wong, W. H. (1987), ‘The calculation of posterior distributions by data augmentation’, *Journal of the American Statistical Association* **82**, 528–540.
- Wang, D., Liu, X. & Chen, R. (2019), ‘Factor models for matrix-valued high-dimensional time series’, *Journal of Econometrics* **208**(1), 231–248.
- Wiśniowski, A., Forster, J. J., Smith, P. W., Bijak, J. & Raymer, J. (2016), ‘Integrated modelling of age and sex patterns of European migration’, *Journal of the Royal Statistical Society Series A: Statistics in Society* **179**(4), 1007–1024.

- Wiśniowski, A., Smith, P. W., Bijak, J., Raymer, J. & Forster, J. J. (2015), ‘Bayesian population forecasting: extending the Lee-Carter method’, *Demography* **52**(3), 1035–1059.
- Yu, R., Chen, R., Xiao, H. & Han, Y. (2024), ‘Dynamic matrix factor models for high dimensional time series’, *arXiv preprint arXiv:2407.05624* .
- Zens, G. (2025), ‘Flexible Bayesian modelling of age-specific counts in many demographic subpopulations’, *Journal of the Royal Statistical Society Series A: Statistics in Society* pp. 1–19, Forthcoming.
- Zens, G. & Bijak, J. (2025), ‘Dynamic Count Models with Flexible Innovation Processes for Irregular Maritime Migration’, *arXiv preprint arXiv:2508.18716* .
- Zens, G., Frühwirth-Schnatter, S. & Wagner, H. (2024), ‘Ultimate Pólya Gamma Samplers—Efficient MCMC for possibly imbalanced binary and categorical data’, *Journal of the American Statistical Association* **119**(548), 2548–2559.
- Zhang, J. L. & Bryant, J. (2020), ‘Bayesian disaggregated forecasts: Internal migration in Iceland’, *Developments in demographic forecasting* pp. 193–215.
- Zhang, W. (2024), ‘Bayesian Dynamic Factor Models for High-dimensional Matrix-valued Time Series’, *arXiv preprint arXiv:2409.08354* .
- Zhao, Q., Zhou, G., Zhang, L., Cichocki, A. & Amari, S.-I. (2015), ‘Bayesian robust tensor factorization for incomplete multiway data’, *IEEE transactions on neural networks and learning systems* **27**(4), 736–748.

SUPPLEMENTARY MATERIAL

S1 Details on Markov Chain Monte Carlo Algorithm

For computing conditional posterior moments, the algorithm makes repeated use of vectorization identities such as

$$\text{vec}(\mathbf{ABC}) = (\mathbf{C}' \otimes \mathbf{A}) \text{vec}(\mathbf{B}) = (\mathbf{I} \otimes \mathbf{AB}) \text{vec}(\mathbf{C}) = (\mathbf{C}'\mathbf{B}' \otimes \mathbf{I}) \text{vec}(\mathbf{A}),$$

where \mathbf{A} , \mathbf{B} , and \mathbf{C} are matrices of appropriate size, \mathbf{I} is the identity matrix, and \otimes denotes the Kronecker product.

Define the matrices $\mathbf{\Omega}_T$ and $\mathbf{\Omega}_A$, which are the usual (first-order) random-walk / ICAR precision matrices on the time and age grids, i.e. intrinsic Gaussian Markov random fields on a one-dimensional chain.⁴ For a generic length- M vector, we use the tridiagonal form

$$\mathbf{\Omega}_M = \begin{bmatrix} 1 & -1 & 0 & \cdots & 0 \\ -1 & 2 & -1 & \ddots & \vdots \\ 0 & -1 & 2 & \ddots & 0 \\ \vdots & \ddots & \ddots & \ddots & -1 \\ 0 & \cdots & 0 & -1 & 1 \end{bmatrix},$$

and set $\mathbf{\Omega}_T = \mathbf{\Omega}_M$ with $M = T$ and $\mathbf{\Omega}_A = \mathbf{\Omega}_M$ with $M = A$. Based on these components, a posterior simulation algorithm can be built by repeatedly iterating through the following steps.

Update latent outcomes $z_{i,t,x}$. For $t = 1, \dots, T$, $x = 1, \dots, A$, and $i = 1, \dots, N$, update

$$z_{i,t,x} \sim p(z_{i,t,x} \mid \cdot) \propto \mathcal{P}(y_{i,t,x}; O_{i,t,x} e^{z_{i,t,x}}) \times \mathcal{N}\left(z_{i,t,x}; \sum_{q=1}^Q \sum_{r=1}^R f_{T,t,q} f_{A,r,x} \lambda_{i,q,r}, \sigma_i^2\right)$$

⁴See, for example, Rue & Held (2005) or Lang & Brezger (2004).

using an appropriate posterior sampling algorithm. We use univariate adaptive Metropolis updates in the style of Roberts & Rosenthal (2009).

Update loading matrices $\mathbf{\Lambda}_i$. For $i = 1, \dots, N$, the updates are based on vectorization of (5), resulting in

$$\text{vec}(\mathbf{Z}_i) = (\mathbf{F}_A \otimes \mathbf{F}_T) \text{vec}(\mathbf{\Lambda}_i) + \text{vec}(\mathbf{E}_i), \quad (\text{S1})$$

which, under multivariate Gaussian priors $\text{vec}(\mathbf{\Lambda}_i) \sim \mathcal{N}(0, \mathbf{L}_{0,i})$, yields a conditional posterior distribution proportional to a multivariate Gaussian $\text{vec}(\mathbf{\Lambda}_i) \sim \mathcal{N}(\mathbf{1}_{N,i}, \mathbf{L}_{N,i})$ with posterior moments

$$\begin{aligned} \mathbf{L}_{N,i} &= \left(\mathbf{L}_{0,i}^{-1} + \frac{1}{\sigma_i^2} (\mathbf{F}_A \otimes \mathbf{F}_T)' (\mathbf{F}_A \otimes \mathbf{F}_T) \right)^{-1}, \\ \mathbf{1}_{N,i} &= \mathbf{L}_{N,i} \left(\frac{1}{\sigma_i^2} (\mathbf{F}_A \otimes \mathbf{F}_T)' \text{vec}(\mathbf{Z}_i) \right). \end{aligned} \quad (\text{S2})$$

Update age factors \mathbf{F}_A . For $r = 1, \dots, R$, the age factors are updated as follows. First, we condition on all age factors other than r by computing the working observations

$$\tilde{\mathbf{Z}}_i = \mathbf{Z}_i - \mathbf{F}_T \mathbf{\Lambda}_i^{-r} (\mathbf{F}_A^{-r})', \quad i = 1, \dots, N,$$

where \mathbf{F}_A^{-r} denotes the $A \times (R - 1)$ matrix obtained by removing column r from \mathbf{F}_A , and $\mathbf{\Lambda}_i^{-r}$ the $Q \times (R - 1)$ loading matrix obtained by removing column r from $\mathbf{\Lambda}_i$.⁵ For each $i = 1, \dots, N$, this results in the regression system

$$\tilde{\mathbf{Z}}_i = \mathbf{F}_T \lambda_{i,\cdot,r} \mathbf{f}'_{A,r} + \mathbf{E}_i, \quad (\text{S3})$$

where $\lambda_{i,\cdot,r}$ denotes the r -th column of $\mathbf{\Lambda}_i$ with dimension $Q \times 1$, and $\mathbf{f}_{A,r}$ is the r -th column

⁵In principle, one could update multiple columns of \mathbf{F}_T and \mathbf{F}_A jointly to improve MCMC mixing. However, the resulting large matrix updates are computationally demanding in high dimensions, so we update factors column-wise, which proved to be an effective compromise between computational cost and mixing in our application.

of \mathbf{F}_A with dimension $A \times 1$. Vectorizing this equation yields

$$\text{vec}(\tilde{\mathbf{Z}}_i) = (\mathbf{I}_A \otimes \mathbf{F}_T \lambda_{i,\cdot,r}) \text{vec}(\mathbf{f}'_{A,r}) + \text{vec}(\mathbf{E}_i). \quad (\text{S4})$$

The r -th age factor $\mathbf{f}_{A,r}$ is then updated based on the stacked regression model

$$\begin{bmatrix} \text{vec}(\tilde{\mathbf{Z}}_1) \\ \vdots \\ \text{vec}(\tilde{\mathbf{Z}}_N) \end{bmatrix} = \begin{bmatrix} \mathbf{I}_A \otimes \mathbf{F}_T \lambda_{1,\cdot,r} \\ \vdots \\ \mathbf{I}_A \otimes \mathbf{F}_T \lambda_{N,\cdot,r} \end{bmatrix} \text{vec}(\mathbf{f}'_{A,r}) + \begin{bmatrix} \text{vec}(\mathbf{E}_1) \\ \vdots \\ \text{vec}(\mathbf{E}_N) \end{bmatrix}. \quad (\text{S5})$$

The resulting conditional posterior distribution is proportional to a multivariate Gaussian $\mathbf{f}_{A,r} \sim \mathcal{N}(\bar{\mathbf{f}}_{A,r}, \bar{\mathbf{F}}_{A,r})$ with posterior moments

$$\begin{aligned} \bar{\mathbf{F}}_{A,r} &= \left(\frac{1}{\tau_{A,r}} \boldsymbol{\Omega}_A + \sum_{i=1}^N \frac{1}{\sigma_i^2} (\mathbf{I}_A \otimes \lambda'_{i,\cdot,r} \mathbf{F}'_T \mathbf{F}_T \lambda_{i,\cdot,r}) \right)^{-1}, \\ \bar{\mathbf{f}}_{A,r} &= \bar{\mathbf{F}}_{A,r} \left(\sum_{i=1}^N \frac{1}{\sigma_i^2} (\mathbf{I}_A \otimes \mathbf{F}_T \lambda_{i,\cdot,r})' \text{vec}(\tilde{\mathbf{Z}}_i) \right). \end{aligned} \quad (\text{S6})$$

Update time factors \mathbf{F}_T . Updating the time factors \mathbf{F}_T is analogous to the column-wise updates of \mathbf{F}_A . For $q = 1, \dots, Q$, the time factors are updated as follows. First, we condition on all time factors other than q by computing the working observations

$$\tilde{\mathbf{Z}}_i = \mathbf{Z}_i - \mathbf{F}_T^{-q} \boldsymbol{\Lambda}_i^{-q} \mathbf{F}'_A, \quad i = 1, \dots, N.$$

Here, \mathbf{F}_T^{-q} denotes the $T \times (Q-1)$ matrix with column q removed and $\boldsymbol{\Lambda}_i^{-q}$ the $(Q-1) \times R$ loading matrix with row q removed. For each $i = 1, \dots, N$, this results in the regression system

$$\tilde{\mathbf{Z}}_i = \mathbf{f}_{T,q} \lambda_{i,q,\cdot} \mathbf{F}'_A + \mathbf{E}_i, \quad (\text{S7})$$

where $\lambda_{i,q,\cdot}$ denotes the q -th row of $\boldsymbol{\Lambda}_i$ with dimension $1 \times R$, and $\mathbf{f}_{T,q}$ is the q -th column of \mathbf{F}_T with dimension $T \times 1$. Vectorizing this equation yields

$$\text{vec}(\tilde{\mathbf{Z}}_i) = (\mathbf{F}_A \lambda'_{i,q,\cdot} \otimes \mathbf{I}_T) \text{vec}(\mathbf{f}_{T,q}) + \text{vec}(\mathbf{E}_i). \quad (\text{S8})$$

The q -th time factor $\mathbf{f}_{T,q}$ is then updated based on the stacked regression model

$$\begin{bmatrix} \text{vec}(\tilde{\mathbf{Z}}_1) \\ \vdots \\ \text{vec}(\tilde{\mathbf{Z}}_N) \end{bmatrix} = \begin{bmatrix} \mathbf{F}_A \lambda'_{1,q} \otimes \mathbf{I}_T \\ \vdots \\ \mathbf{F}_A \lambda'_{N,q} \otimes \mathbf{I}_T \end{bmatrix} \text{vec}(\mathbf{f}_{T,q}) + \begin{bmatrix} \text{vec}(\mathbf{E}_1) \\ \vdots \\ \text{vec}(\mathbf{E}_N) \end{bmatrix}. \quad (\text{S9})$$

The resulting conditional posterior distribution is proportional to a multivariate Gaussian $\mathbf{f}_{T,q} \sim \mathcal{N}(\bar{\mathbf{f}}_{T,q}, \bar{\mathbf{F}}_{T,q})$ with posterior moments

$$\begin{aligned} \bar{\mathbf{F}}_{T,q} &= \left(\frac{1}{\tau_{T,q}} \boldsymbol{\Omega}_T + \sum_{i=1}^N \frac{1}{\sigma_i^2} (\lambda_{i,q}, \mathbf{F}'_A \mathbf{F}_A \lambda'_{i,q} \otimes \mathbf{I}_T) \right)^{-1}, \\ \bar{\mathbf{f}}_{T,q} &= \bar{\mathbf{F}}_{T,q} \left(\mathbf{h}_{0,q} + \sum_{i=1}^N \frac{1}{\sigma_i^2} (\mathbf{F}_A \lambda'_{i,q} \otimes \mathbf{I}_T)' \text{vec}(\tilde{\mathbf{Z}}_i) \right), \end{aligned} \quad (\text{S10})$$

where the term $\mathbf{h}_{0,q}$ captures the contribution of the random walk with drift prior,

$$\mathbf{h}_{0,q} = \frac{\kappa_q}{\tau_{T,q}} (-1, 0, \dots, 0, 1)'. \quad (\text{S11})$$

This follows directly from writing

$$f_{T,t,q} = \kappa_q + f_{T,t-1,q} + \eta_{T,t,q}, \quad \eta_{T,t,q} \sim \mathcal{N}(0, \tau_{T,q}),$$

in terms of first differences $\Delta f_{T,t,q} = f_{T,t,q} - f_{T,t-1,q} \sim \mathcal{N}(\kappa_q, \tau_{T,q})$. Stacking over t with the first-difference matrix \mathbf{D}_T and $\mathbf{1}_{T-1}$ a vector of ones gives

$$p(\mathbf{f}_{T,q} \mid \kappa_q, \tau_{T,q}) \propto \exp\left(-\frac{1}{2\tau_{T,q}} \|\mathbf{D}_T \mathbf{f}_{T,q} - \kappa_q \mathbf{1}_{T-1}\|^2\right).$$

Expanding the quadratic form yields

$$-\frac{1}{2} \mathbf{f}'_{T,q} \left(\frac{1}{\tau_{T,q}} \boldsymbol{\Omega}_T \right) \mathbf{f}_{T,q} + \mathbf{f}'_{T,q} \left(\frac{\kappa_q}{\tau_{T,q}} \mathbf{D}'_T \mathbf{1}_{T-1} \right),$$

so the prior contributes precision $(1/\tau_{T,q})\boldsymbol{\Omega}_T$ and canonical mean $\mathbf{h}_{0,q} = (\kappa_q/\tau_{T,q})\mathbf{D}'_T \mathbf{1}_{T-1} = (\kappa_q/\tau_{T,q})(-1, 0, \dots, 0, 1)'$, as stated above.

Update drift parameters κ_q . For $q = 1, \dots, Q$, the conditional posterior densities $p(\kappa_q \mid \mathbf{f}_{T,q}, \tau_{T,q})$ are proportional to Gaussian densities $\kappa_q \sim \mathcal{N}(\bar{\kappa}_q, V_{\kappa,q})$ with posterior moments

$$V_{\kappa,q} = \frac{\tau_{T,q}}{T-1}, \quad \bar{\kappa}_q = \frac{1}{T-1} \sum_{t=2}^T (f_{T,t,q} - f_{T,t-1,q}). \quad (\text{S12})$$

Update smoothing parameters τ_T and τ_A . For $r = 1, \dots, R$ and $q = 1, \dots, Q$, the conditional posterior densities $p(\tau_{T,q} \mid \mathbf{f}_{T,q}) \propto \mathcal{IG}(d_{N,q}, D_{N,q})$ and $p(\tau_{A,r} \mid \mathbf{f}_{A,r}) \propto \mathcal{IG}(d_{N,r}, D_{N,r})$ are proportional to inverse-gamma densities with posterior moments

$$\begin{aligned} d_{N,q} &= \frac{1}{2}(T-1), \\ D_{N,q} &= \frac{1}{2} \sum_{t=2}^T (f_{T,t,q} - \kappa_q - f_{T,t-1,q})^2, \\ d_{N,r} &= \frac{1}{2}(A-1), \\ D_{N,r} &= \frac{1}{2} \sum_{x=2}^A (f_{A,r,x} - f_{A,r,x-1})^2. \end{aligned} \quad (\text{S13})$$

Update observation equation error variances σ_i^2 . The conditional posterior distributions $p(\sigma_i^2 \mid \mathbf{Z}, \mathbf{F}_A, \mathbf{F}_T, \mathbf{\Lambda}) \propto \mathcal{IG}(c_{N,i}, C_{N,i})$ are proportional to inverse-gamma densities with posterior moments

$$\begin{aligned} c_{N,i} &= c_0 + \frac{1}{2}AT, \\ C_{N,i} &= C_0 + \frac{1}{2} \sum_{t=1}^T \sum_{x=1}^A \left(z_{i,t,x} - \sum_{r=1}^R \sum_{q=1}^Q f_{T,t,q} f_{A,r,x} \lambda_{i,q,r} \right)^2. \end{aligned} \quad (\text{S14})$$

S2 Simulation Experiment

To assess the ability of the proposed MCMC algorithm to recover the underlying parameters, we conduct a controlled simulation study in which data are generated from the matrix factor model in Sec. 4. We simulate $N = 50$ subpopulations observed over $T = 30$ time points and $A = 40$ single-year age groups. We set the number of time and age factors to $Q = 3$ and $R = 3$. Time factors are generated from random-walk-with-drift dynamics,

$$f_{T,0,q} \sim \mathcal{N}(0, \tau_{T,q}), \quad f_{T,t,q} = \kappa_q + f_{T,t-1,q} + \eta_{T,t,q}, \quad \eta_{T,t,q} \sim \mathcal{N}(0, \tau_{T,q}),$$

for $t = 1, \dots, T$ and $q = 1, \dots, Q$, with $\boldsymbol{\tau}_T = (0.01, 0.02, 0.03)$ and $\boldsymbol{\kappa} = (-0.05, 0.05, 0)$.

Age factors are generated as first-order random walks in age,

$$f_{A,0,r} \sim \mathcal{N}(0, \tau_{A,r}), \quad f_{A,x,r} = f_{A,x-1,r} + \zeta_{A,x,r}, \quad \zeta_{A,x,r} \sim \mathcal{N}(0, \tau_{A,r}),$$

for $x = 1, \dots, A$ and $r = 1, \dots, R$, with $\boldsymbol{\tau}_A = (0.01, 0.02, 0.03)$. For each subpopulation $i = 1, \dots, N$, we draw the loading matrix $\boldsymbol{\Lambda}_i$ element-wise from a standard normal distribution,

$$\lambda_{i,q,r} \sim \mathcal{N}(0, 1), \quad q = 1, \dots, Q, \quad r = 1, \dots, R.$$

Conditional on $(\mathbf{F}_T, \mathbf{F}_A, \boldsymbol{\Lambda}_i)$, the true latent conditional means and latent Gaussian variables are given by

$$\mathbf{Z}_i^* = \mathbf{F}_T \boldsymbol{\Lambda}_i \mathbf{F}_A', \quad \mathbf{Z}_i = \mathbf{Z}_i^* + \mathbf{E}_i,$$

where the elements of \mathbf{E}_i are assumed to be iid $\mathcal{N}(0, \sigma_i^2)$ and the error variances σ_i^2 are simulated iid from $\mathcal{IG}(10, 1)$. Finally, we fix the offsets $O_{i,t,x} = 10$ for all i, t, x and generate Poisson counts from

$$y_{i,t,x} \mid O_{i,t,x}, z_{i,t,x} \sim \mathcal{P}(O_{i,t,x} \exp(z_{i,t,x})), \quad t = 1, \dots, T, \quad x = 1, \dots, A, \quad i = 1, \dots, N.$$

We then fit the proposed model to the simulated counts using the known factor dimensions $Q = 3$ and $R = 3$, iterating the MCMC algorithm for 25,000 draws after an initial

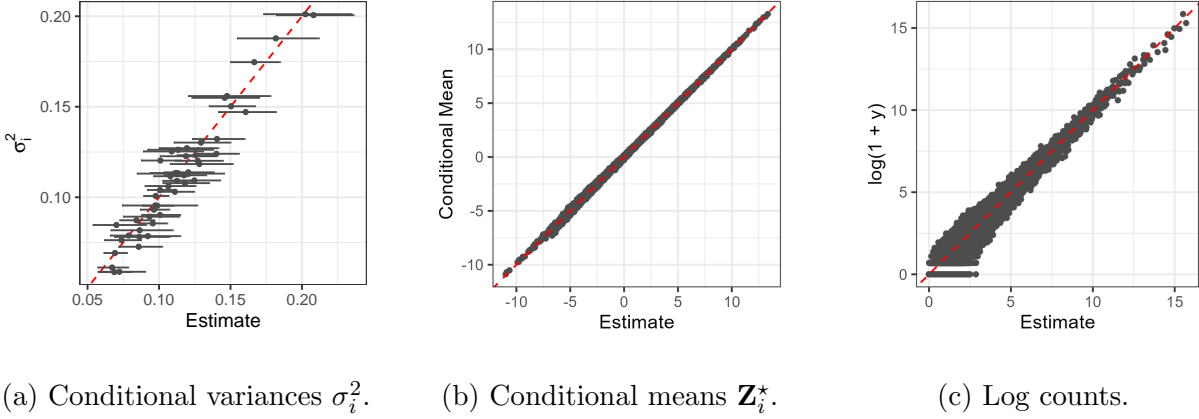
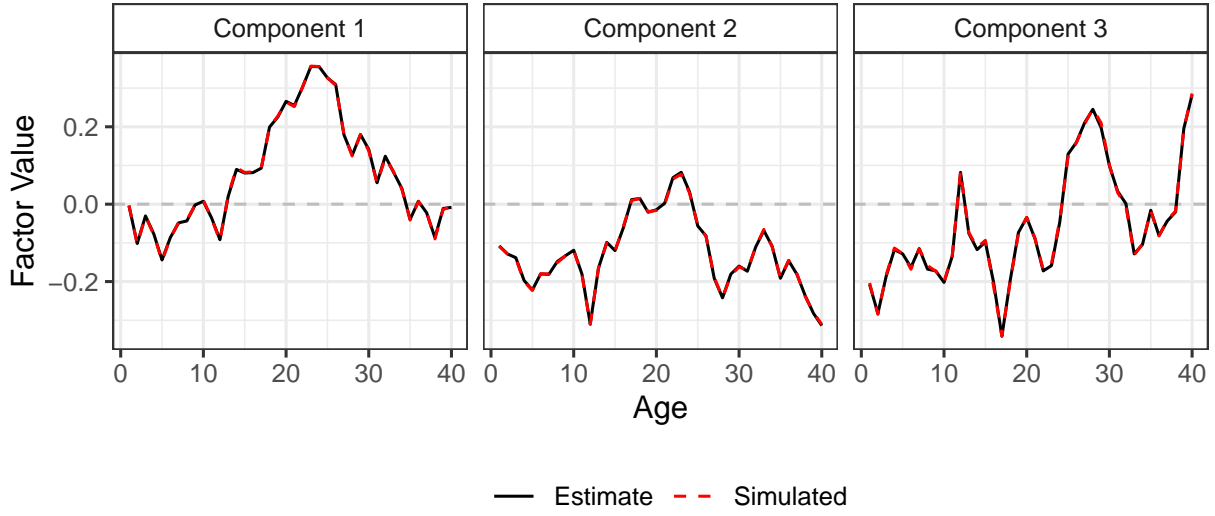
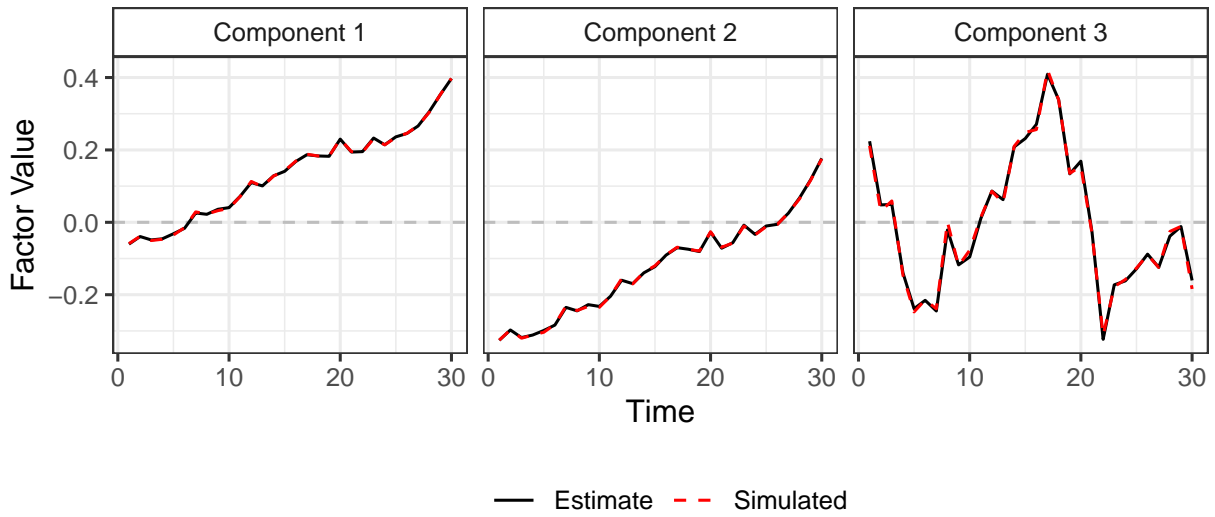


Figure S1: Recovery of conditional variances (a), conditional means (b) and counts on the $\log(1 + y)$ scale (c). Dashed red lines indicate the 45-degree reference line.

burn-in period of 7,500 iterations. To evaluate parameter recovery, we compare posterior summaries to the known data-generating values. Fig. S1 summarizes recovery of identified structures such as the conditional mean and conditional variance of \mathbf{Z}_i . Panel (a) compares posterior means and 95% credible intervals for the population-specific variances σ_i^2 against the true values. Panel (b) compares fitted conditional means to the simulated conditional means \mathbf{Z}_i^* , while panel (c) compares posterior predictive means for the counts with the observed counts on the $\log(1 + y)$ scale. Fig. S2 displays the simulated and estimated age and time factors obtained from an ex post HOSVD of the true \mathbf{Z}_i^* and of the posterior mean fitted values $\mathbb{E}[\mathbf{Z}_i | \mathbf{Y}]$, corresponding to the procedure described in Sec. 5 and used to produce Fig. S3. Overall, the agreement between simulated and recovered quantities is satisfactory, bearing in mind that these results are based on a single simulation run, so some sampling variation is to be expected.



(a) Age factors



(b) Time factors

Figure S2: Simulated (red) and estimated (black) age factors (a) and time factors (b) for components $r, q = 1, 2, 3$, obtained from a post-hoc HOSVD of the simulated and fitted conditional means.

S3 Details on Benchmark Forecasting Models

This section provides implementation details for the competing models used in the forecasting exercise in Sec. 5. All models are fitted to and evaluated on transformed log-counts $\tilde{y}_{i,t,x} = \log(1 + y_{i,t,x})$. For each of the five rolling hold-out splits described in the main text (17-year training window and 1-year hold-out; plus an additional 5-year-ahead evaluation for the first split), we generate point forecasts $\hat{y}_{i,t+h,x}$ for horizons $h = 1$ and, where applicable, $h = 5$.

S3.1 Univariate Random Walk Benchmarks

Random walk. For each age x and subpopulation i , we estimate a univariate random walk on the transformed series $\{\tilde{y}_{i,t,x}\}_{t=1}^T$,

$$\tilde{y}_{i,t,x} = \tilde{y}_{i,t-1,x} + \varepsilon_{i,t,x}, \quad \varepsilon_{i,t,x} \sim \mathcal{N}(0, \sigma_{i,x}^2).$$

Random walk with drift. The second benchmark augments the random walk with a constant drift term,

$$\tilde{y}_{i,t,x} = \delta_{i,x} + \tilde{y}_{i,t-1,x} + \varepsilon_{i,t,x}, \quad \varepsilon_{i,t,x} \sim \mathcal{N}(0, \sigma_{i,x}^2).$$

S3.2 Time Factorization Models

Let $\tilde{\mathbf{Y}}_i$ denote the $T \times A$ matrix with elements $\tilde{y}_{i,t,x}$ in rows t and columns x . The time-factorization benchmarks approximate the (log-transformed) data using a small number of time factors with age–population-specific loadings, and then forecast the time factors as random walks with drift.

Separate time factorization. For each subpopulation i separately, we consider the transpose of the log-count matrix $\mathbf{D}_i = \tilde{\mathbf{Y}}'_i \in \mathbb{R}^{A \times T}$ and compute a singular value decomposition (after row-wise centering and scaling) $\mathbf{D}_i \approx \mathbf{U}_i \mathbf{S}_i \mathbf{V}'_i$, where \mathbf{V}_i is $T \times T$. The first Q columns of \mathbf{V}_i are taken as estimated time factors for subpopulation i , $\mathbf{f}_{i,t} = (f_{i,t,1}, \dots, f_{i,t,Q})'$. For each age x and subpopulation i , we then fit the linear regression

$$\tilde{y}_{i,t,x} = \alpha_{i,x} + \sum_{q=1}^Q \beta_{i,x,q} f_{i,t,q} + \varepsilon_{i,t,x}, \quad \varepsilon_{i,t,x} \sim \mathcal{N}(0, \sigma_{i,x}^2).$$

The dynamic component is captured by the time factors. For each q , the factor series $\{f_{i,t,q}\}_{t=1}^T$ is forecast using a random walk with drift,

$$f_{i,t,q} = \delta_{i,q} + f_{i,t-1,q} + \eta_{i,t,q}, \quad \eta_{i,t,q} \sim \mathcal{N}(0, \tau_{i,q}^2).$$

Denote the h -step-ahead factor forecast by $\hat{\mathbf{f}}_{i,T+h}$; the resulting forecast for the log-count at age x is $\hat{y}_{i,T+h,x} = \hat{\alpha}_{i,x} + \sum_{q=1}^Q \hat{\beta}_{i,x,q} \hat{f}_{i,T+h,q}$.

Joint time factorization. The joint time factorization shares the time factors across all age–subpopulation series. We first matricize the full training array $\tilde{\mathbf{Y}}$ along the time mode, obtaining a matrix $\mathbf{D} \in \mathbb{R}^{(AN) \times T}$ whose rows correspond to all age–subpopulation combinations and whose columns correspond to time. After row-wise centering and scaling, we compute the SVD $\mathbf{D} \approx \mathbf{U} \mathbf{S} \mathbf{V}'$ and use the first Q columns of \mathbf{V} as joint time factors $\mathbf{f}_t = (f_{t,1}, \dots, f_{t,Q})'$, common to all series. For each row j of \mathbf{D} (i.e., each age–subpopulation combination), we estimate

$$\tilde{y}_{j,t} = \alpha_j + \sum_{q=1}^Q \beta_{j,q} f_{t,q} + e_{j,t},$$

by ordinary least squares. As before, each factor $f_{t,q}$ is forecast using a random walk with drift, yielding $\hat{\mathbf{f}}_{T+h}$, and the corresponding log-count forecast is $\hat{y}_{j,T+h} = \hat{\alpha}_j + \sum_{q=1}^Q \hat{\beta}_{j,q} \hat{f}_{T+h,q}$.

S3.3 Age Factorization Models

The age-factorization benchmarks summarize the cross-sectional age profiles at each time point by a small number of age factors with time–population-specific loadings, and then forecast the loadings as random walks with drift.

Separate age factorization. For each subpopulation i separately, we use the $T \times A$ log-count matrix $\tilde{\mathbf{Y}}_i$ and compute an SVD (after row-wise centering and scaling) $\tilde{\mathbf{Y}}_i \approx \mathbf{U}_i \mathbf{S}_i \mathbf{V}_i'$, where \mathbf{V}_i is $A \times A$. The first R columns of \mathbf{V}_i form the subpopulation-specific age factor matrix $\mathbf{F}_{i,A} = [\mathbf{f}_{i,A,1}, \dots, \mathbf{f}_{i,A,R}] \in \mathbb{R}^{A \times R}$. For each time t , the age profile $\tilde{\mathbf{y}}_{i,t} = (\tilde{y}_{i,t,1}, \dots, \tilde{y}_{i,t,A})'$ is then approximated as

$$\tilde{\mathbf{y}}_{i,t} \approx \alpha_i \mathbf{1}_A + \mathbf{F}_{i,A} \boldsymbol{\beta}_{i,t},$$

where α_i is a subpopulation-specific intercept, $\mathbf{1}_A$ is an A -vector of ones, and $\boldsymbol{\beta}_{i,t} = (\beta_{i,1,t}, \dots, \beta_{i,R,t})'$ is a vector of time-varying loadings. All $\boldsymbol{\beta}_{i,t}$ are estimated using least squares regression. For each factor $r = 1, \dots, R$, the loading series $\{\beta_{i,r,t}\}_{t=1}^T$ is then forecast using a random walk with drift,

$$\beta_{i,r,t} = \delta_{i,r} + \beta_{i,r,t-1} + \xi_{i,r,t}, \quad \xi_{i,r,t} \sim \mathcal{N}(0, \omega_{i,r}^2),$$

producing forecasts $\hat{\boldsymbol{\beta}}_{i,T+h}$. The age-specific log-count forecast is $\hat{\tilde{\mathbf{y}}}_{i,T+h} = \hat{\alpha}_i \mathbf{1}_A + \mathbf{F}_{i,A} \hat{\boldsymbol{\beta}}_{i,T+h}$.

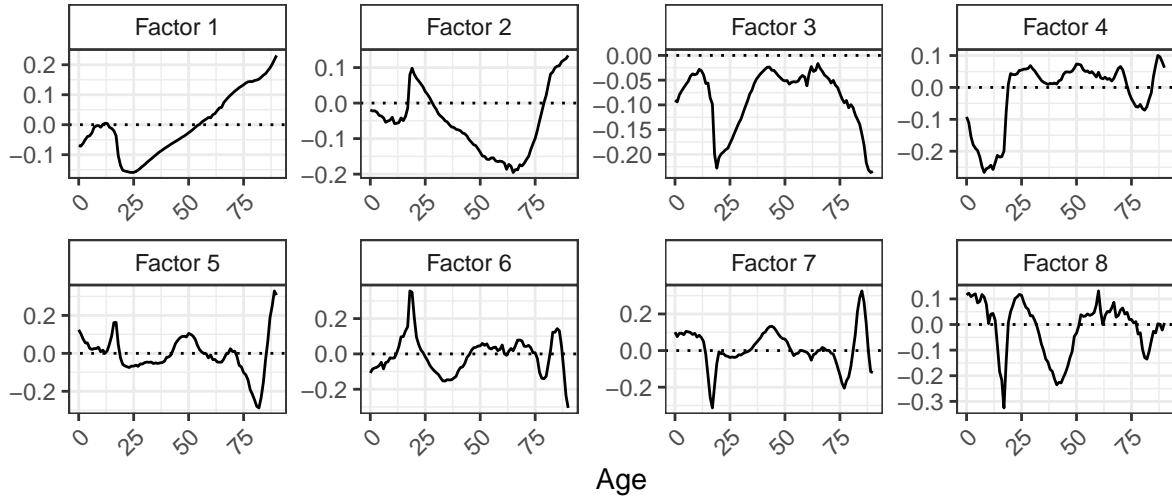
Joint age factorization. The joint age factorization shares the age factors across all subpopulations. We first matricize the full training array along the age mode, yielding $\mathbf{D}_{\text{age}} \in \mathbb{R}^{(TN) \times A}$, whose rows correspond to all time–subpopulation combinations and whose columns correspond to age. After row-wise centering and scaling, we compute the SVD $\mathbf{D}_{\text{age}} \approx \mathbf{U} \mathbf{S} \mathbf{V}'$ and take the first R columns of \mathbf{V} as a set of joint age factors $\mathbf{F}_A =$

$[\mathbf{f}_{A,1}, \dots, \mathbf{f}_{A,R}] \in \mathbb{R}^{A \times R}$ common to all subpopulations. For each subpopulation i , we then approximate the age profile at time t as

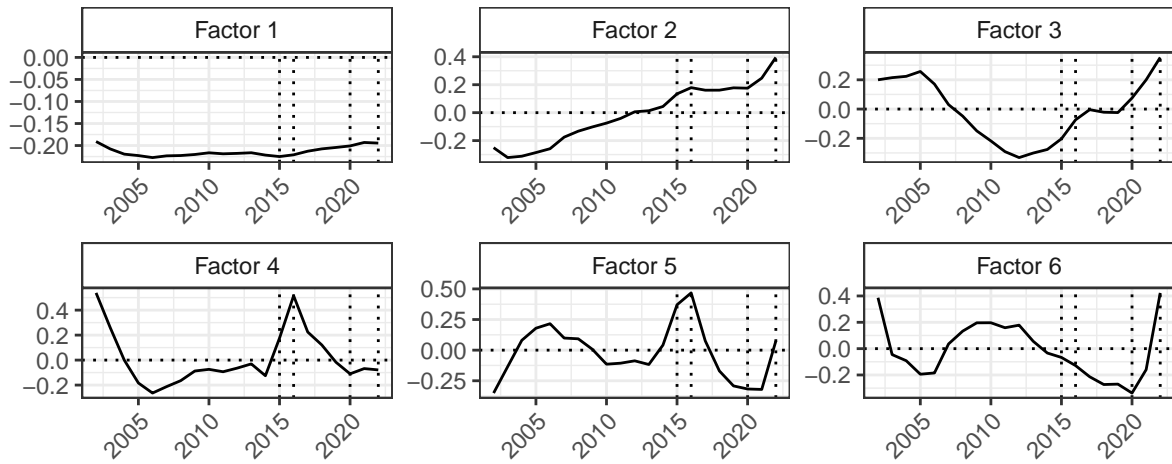
$$\tilde{\mathbf{y}}_{i,t} \approx \alpha_i \mathbf{1}_A + \mathbf{F}_A \boldsymbol{\beta}_{i,t},$$

where $\boldsymbol{\beta}_{i,t}$ is estimated using least squares regression. The loadings $\{\beta_{i,r,t}\}_{t=1}^T$ are forecast as random walks with drift for each factor r , and the age-specific log-count forecasts are given by $\hat{\mathbf{y}}_{i,T+h} = \hat{\alpha}_i \mathbf{1}_A + \mathbf{F}_A \hat{\boldsymbol{\beta}}_{i,T+h}$.

S4 Additional Figures



(a) Age Factors.



(b) Time Factors.

Figure S3: HOSVD-based factor estimates at the posterior mean of $\mathbf{F}_T \mathbf{\Lambda}_i \mathbf{F}'_A$ for age (a) and time (b) modes. Horizontal dotted line indicates zero. Vertical dotted lines indicate the years 2015, 2016, 2020 and 2022.

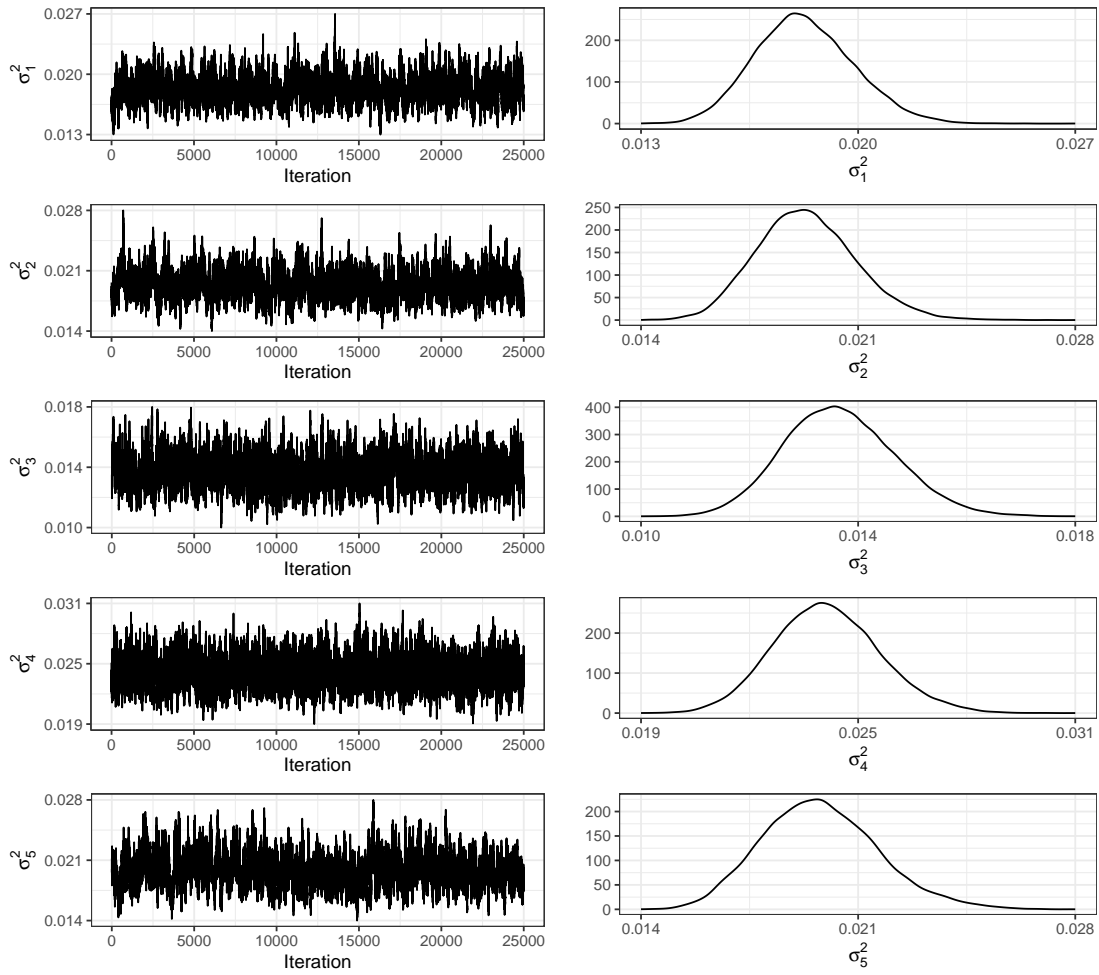
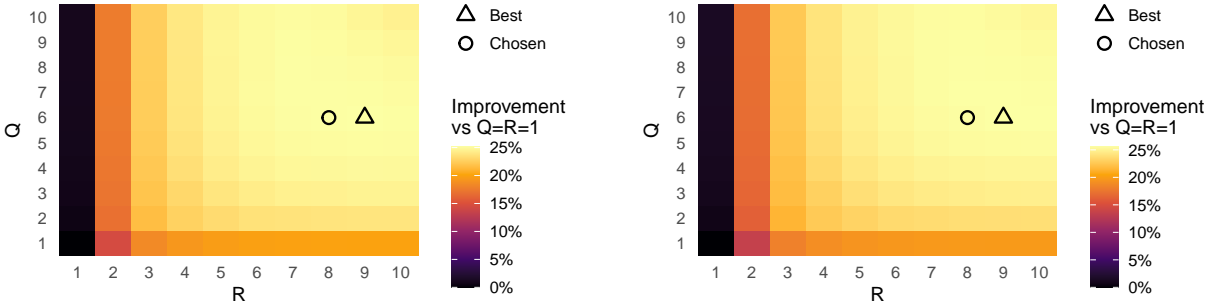
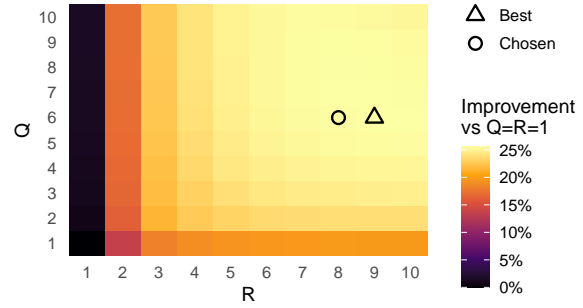


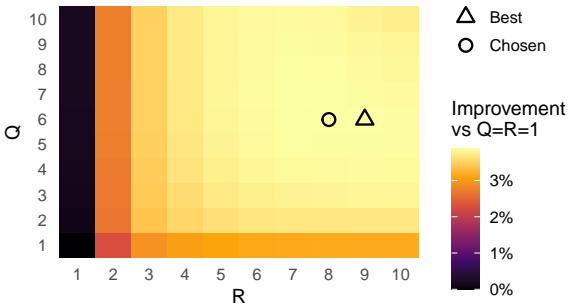
Figure S4: Traceplots and posterior distributions, row-wise corresponding to σ_i^2 for the first five populations in the data.



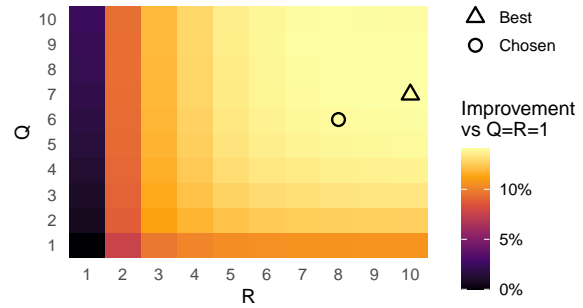
(a) RMSE.



(b) MAE.



(c) Correlation.



(d) LPS.

Figure S5: Ten-fold cross-validation performance across (Q, R) combinations. Colors show relative change in each metric compared to the baseline setting $Q = R = 1$, with higher values indicating better performance. RMSE = Root Mean Squared Error, MAE = Mean Absolute Error, Corr. = Correlation Coefficient, LPS = Log Predictive Score. Points mark the chosen model $(Q, R) = (6, 8)$ and triangles mark best model for each metric.